The Referred Weight Flight Test Technique Applied to First of Class Flight Trials

A.M. Arney

DEPARTMENT OF DEFENCE
DEFENCE SCIENCE AND TECHNOLOGY ORGANISATION

The Referred Weight Flight Test Technique Applied to First of Class Flight Trials

A.M. Arney

Air Operations Division
Aeronautical and Maritime Research Laboratory

DSTO-TR-0509

ABSTRACT

The referred weight flight test technique has been used by the RAN to establish Ship Helicopter Operating Limits for a number of years. This technique involves keeping the referred weight, defined as aircraft weight divided by density ratio, constant for a given flight test. The validity of using this technique has been questioned within the RAN, specifically with respect to its relevance and application to power and flight control margins. This report illustrates the relationships between power requirements, flight control positions, and referred weight by first using simplified equations to derive the mathematical relationships. To verify these relationships, the simulation code *GenHel*, which allows for many of the complex factors ignored in deriving the simplified equations, has been applied over a wide range of conditions. Results suggest that the referred weight technique is valid for conditions typically encountered during First of Class Flight Trials.

RELEASE LIMITATION

Approved for public release

DEPARTMENT OF DEFENCE

DEFENCE SCIENCE AND TECHNOLOGY ORGANISATION

Published by

DSTO Aeronautical and Maritime Research Laboratory
PO Box 4331
Melbourne Victoria 3001

Telephone: (03) 9626 7000
Fax: (03) 9626 7999

AR-010-178
April 1997

APPROVED FOR PUBLIC RELEASE

The Referred Weight Flight Test Technique Applied to First of Class Flight Trials

Executive Summary

From 4 to 30 March 1994, the First of Class Flight Trial (FOCFT) for the S-70B-2 helicopter on the 'Adelaide' class of FFG-7 frigate was conducted aboard HMAS SYDNEY. The aircraft was instrumented to record flight control positions and flight dynamic parameters. The ship was instrumented to record motion and relative wind velocity parameters. The purpose of this trial was to develop new Ship Helicopter Operating Limits (SHOLs) for operational use. This trial was performed by the Aircraft Maintenance and Flight Trials Unit (AMAFTU) of the Royal Australian Navy (RAN) with the aid of Air Operations Division (AOD) of the Defence Science and Technology Organisation (DSTO).

SHOLs are usually developed for a range of operating weights, both day and night, for a defined standard atmosphere. If the actual atmospheric conditions (i.e. ambient atmospheric pressure and air temperature) on a given day are not identical to the atmospheric conditions for which the SHOLs were developed, weight corrections must be applied. The International Standard Atmosphere (ISA) is defined as having a temperature of 15°C (288.15 K), at sea-level. Applying weight corrections for any day with temperatures higher than 15°C is restrictive to the RAN, given that most flying in Australia's region is conducted in conditions warmer than ISA. By using an atmosphere based on ISA+5°C conditions, weight corrections need not be applied until the sea-level temperature rises above 20°C.

The referred weight (defined as weight divided by density ratio, W/σ_ρ) technique has been widely used during First of Class Flight Trials (FOCFTs) for many years. The objective of this technique is to ensure that a set of tests conducted for one particular atmospheric condition can be directly comparable with another set of tests conducted under different atmospheric conditions. This will provide data which can be referred to the non-standard day conditions which generally occur during normal operations. The validity of using this technique has been questioned within the RAN, specifically with respect to its relevance and application to power and flight control margins, although use of the technique with the ISA as the reference has been well established for performance tests. In addition, AMAFTU have recently begun using an ISA+5°C atmosphere as the reference so that weight corrections need not be applied until this condition has been exceeded. AOD was asked to confirm the validity of the W/σ_ρ technique when applied to developing SHOLs and that using an off-standard atmosphere as the reference would not invalidate the W/σ_ρ technique.

This report illustrates the relationships between power requirements, control positions, and W/σ_ρ by first using simplified equations to derive the mathematical relationships. To demonstrate that the simplified equations are valid, the simulation code *GenHel*, acquired from the US through The Technical Collaboration Program (TTCP), has been applied over a wide range of conditions typically encountered during a FOCFT. This code is optimised for the S70 family of helicopters and allows for many of the complex factors that were ignored in deriving the simplified equations. *GenHel* has been shown to model measured flight data reasonably well although factors such as ship airwake effects are not modelled. Results suggest that the W/σ_ρ technique is valid for conditions typically encountered during First of Class Flight Trials.

The Defence outcome of this work is progress towards safe definitions of the operational capability of maritime helicopters in embarked operations.

Authors

A.M. Arney
Air Operations Division

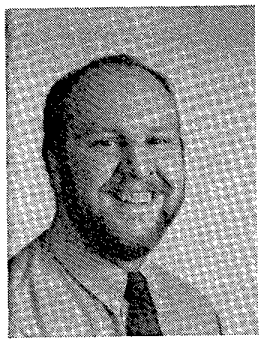

Ashley Arney graduated from the University of Sydney in 1981, having obtained an Aeronautical Engineering Degree, with honours. Since commencing employment at the then Aeronautical Research Laboratory in 1982, he has been involved with the mathematical modelling of the performance and flight dynamics of a wide range of helicopters. He has also obtained extensive experience in trials, data processing, and the use of such data for development of models. More recently he has been involved in modelling the helicopter-ship dynamic interface, and gathering data for development purposes.

CONTENTS

NOMENCLATURE

a blade section lift-curve slope

a_s speed of sound

b number of rotor blades

c rotor blade chord

f fuselage equivalent flat plate area

g gravitational acceleration

h_d density altitude

h_p pressure altitude

l_{tr} distance from main rotor centre of rotation to tail rotor centre of thrust

s standard deviation

$\bar{x}$ mean

A_{1s} main rotor lateral cyclic blade angle in shaft axes

B_{1s} main rotor longitudinal cyclic blade angle in shaft axes

C_{d_o} mean rotor profile drag coefficient

C_T thrust coefficient $\left(\frac{T}{\rho\pi R^2(\Omega R)^2}\right)$

L standard atmospheric temperature lapse rate

P total power required

P_a ambient air pressure

P_{acc} power required to drive accessories

P_i induced power (power required to generate lift)

P_{mr} main rotor power required

P_o profile power (power required to overcome rotor blade drag)

P_p parasite power (power required to overcome aircraft drag)

P_{SL} reference sea-level air pressure

P_{tr} tail rotor total power required

Q total torque

Q_{mr} main rotor torque

R rotor blade radius

R_g gas constant for air

T rotor thrust

T_a ambient air temperature

T_{SL} reference sea-level air temperature

V true airspeed

V_{eq} equivalent airspeed

W aircraft weight

Ω rotor angular velocity

α angle of attack of Axis of No Feathering (= angle of attack of Tip Path Plane in hover)

δ pressure ratio or relative pressure (P_a/P_{SL})

θ temperature ratio or relative temperature (T_a/T_{SL})

θ_o blade root collective pitch

θ_l blade linear twist

λ inflow ratio $\left(\frac{V\sin\alpha - v}{\Omega R}\right)$

μ advance ratio $\left(\frac{V\cos\alpha}{\Omega R}\right)$

v induced velocity

v_h induced velocity at hover

ρ ambient air density

ρ_{SL} reference sea-level air density

σ rotor solidity ratio ($bc/\pi R$)

σ_ρ density ratio or relative density (ρ/ρ_{SL})

ϕ Euler roll attitude

Additional subscripts

max maximum value

min minimum value

mr main rotor

tr tail rotor

ISA International Standard Atmosphere conditions

ISA+5 International Standard Atmosphere conditions with an increase in T_a of 5°C

SL sea level

1. INTRODUCTION

From 4 to 30 March 1994, the First of Class Flight Trial (FOCFT) for the S-70B-2 helicopter on the 'Adelaide' class of FFG-7 frigate was conducted aboard HMAS SYDNEY (Ref. 1). The aircraft was instrumented to record flight control positions and flight dynamic parameters. The ship was instrumented to record motion and relative wind velocity parameters. The purpose of this trial was to develop new Ship Helicopter Operating Limits (SHOLs) for operational use. This trial was performed by the Aircraft Maintenance and Flight Trials Unit (AMAFTU) of the Royal Australian Navy (RAN) with the aid of Air Operations Division (AOD) of the Defence Science and Technology Organisation (DSTO).

SHOLs are usually developed for a range of operating weights, both day and night, for a defined standard atmosphere. If the actual atmospheric conditions (i.e. ambient atmospheric pressure and air temperature) on a given day are not identical to the atmospheric conditions for which the SHOLs were developed, weight corrections must be applied. The International Standard Atmosphere (ISA) is defined as having a temperature of 15°C (288.15 K), at sea-level. Applying weight corrections for any day with temperatures higher than 15°C is restrictive to the RAN, given that most flying in Australia's region is conducted in conditions warmer than ISA. By using an atmosphere based on ISA+5°C conditions, weight corrections need not be applied until the sea-level temperature rises above 20°C.

The referred weight (defined as weight divided by density ratio, W/σ_ρ) technique has been widely used during FOCFTs for many years (Refs 1 to 4) and normalises the aircraft weight to a standard air density. The objective of this technique is to ensure that a set of tests conducted for one particular atmospheric condition can be directly comparable with another set of tests conducted under different atmospheric conditions, i.e. referred to a standard. This will provide data which can be referred to the non-standard day conditions which generally occur during normal operations. The validity of using this technique has been questioned within the RAN, specifically with respect to its relevance and application to power and flight control margins, although use of the technique with the ISA as the reference has been well established for performance tests (Ref. 5). In addition, AMAFTU have recently begun using an ISA+5°C atmosphere as the reference so that weight corrections need not be applied until this condition has been exceeded (Refs 1 and 2). AOD was asked to confirm the validity of the W/σ_ρ technique when applied to developing SHOLs and also confirm that using an off-standard atmosphere as the reference would not invalidate the W/σ_ρ technique.

This report illustrates the relationships between power requirements, control positions, and W/σ_ρ by first using simplified equations to derive the mathematical relationships. To demonstrate that the simplified equations are valid, the simulation code *GenHel* (Refs 6 and 7), acquired from the US through The Technical Collaboration Program (TTCP), has been applied over a wide range of conditions typically encountered during a FOCFT. This code is optimised for the S70 family of helicopters and allows for many of the complex factors that were ignored in deriving the simplified equations. *GenHel* has been shown to model measured flight data reasonably well (Refs 8 to 10) although factors such as ship airwake effects are not modelled.

2. REFERRED POWER REQUIRED

The total power required consists of main rotor power, tail rotor power, and accessories, where the allowance for accessories accounts for gearbox transmission losses as well as electronics, heating, cooling, etc.

$$P = P_{mr} + P_{tr} + P_{acc}$$

where P is the total power required, P_{mr} and P_{tr} are the main and tail rotor powers required respectively, and P_{acc} is the power required to drive accessories. For a given airspeed, the tail rotor power required can be expressed as a constant proportion of the total power required (xP). Also, the power requirement for the accessories can be given as a constant proportion of the total power required (yP). Thus

$$P = P_{mr} + xP + yP$$
$$= \frac{1}{1-x-y} P_{mr}$$

where x and y each are less than 1. Thus for a given airspeed

$$P = k_0 P_{mr}$$

where $k_0 > 1$.

Thus, when considering the power margin at a given airspeed, the power required by the main rotor need only be considered. For the main rotor

$$P_{mr} = P_i + P_o + P_p$$

where P_i is the induced power, P_o is the profile power, and P_p is the parasite power.

Now, from Ref. 11, P_i, P_o, and P_p may be given by

$$P_i = Tv$$

where T is the rotor thrust and v is the induced velocity.

$$P_o = \frac{\sigma\, C_{d_o}}{8} \rho \pi R^2 (\Omega R)^3 \left(1 + 4.3\mu^2\right)$$

where σ is the rotor solidity ratio ($\sigma = bc/\pi R$, where b is the number of rotor blades, c is the blade chord, and R is the rotor radius), C_{d_o} is the mean rotor profile drag coefficient, ρ is the ambient air density, Ω is the rotor angular velocity, and μ is the advance ratio ($= V\cos\alpha / \Omega R$, where V is the true airspeed and α is the angle of attack of the Axis of No Feathering).

$$P_p = \frac{1}{2} \rho V^3 f$$

where f is the fuselage equivalent flat plate area.

Thus

$$P_{mr} = Tv + \frac{\sigma\, C_{d_o}}{8} \rho \pi R^2 (\Omega R)^3 \left(1 + 4.3\mu^2\right) + \frac{1}{2} \rho V^3 f \qquad (1)$$

At low speeds, α is small and thus $\mu \approx V/\Omega R$. For a given helicopter, σ and R are constant. As a first approximation, C_{d_o} and f can be assumed to be constant, although both will change with variation in α. Also, assuming constant rotor speed, equation (1) becomes

$$P_{mr} = Tv + k_1 \rho \left(1 + k_2 V^2\right) + k_3 \rho V^3 \qquad (2)$$

where $k_1 = \frac{\sigma\, C_{d_o}}{8} \pi R^2 (\Omega R)^3$, $k_2 = \frac{4.3}{(\Omega R)^2}$, and $k_3 = \frac{f}{2}$

Dividing equation (2) by ρ gives

$$\frac{P_{mr}}{\rho} = \frac{T}{\rho} v + k_1\left(1 + k_2 V^2\right) + k_3 V^3 \tag{3}$$

and multiplying both sides by ρ_{SL} (reference sea level air density)

$$\frac{P_{mr}}{\rho/\rho_{SL}} = \left(\frac{T}{\rho/\rho_{SL}}\right) v + k_1\rho_{SL}\left(1 + k_2 V^2\right) + k_3\rho_{SL} V^3$$

or

$$\frac{P_{mr}}{\sigma_\rho} = \left(\frac{T}{\sigma_\rho}\right) v + k_4\left(1 + k_2 V^2\right) + k_5 V^3 \tag{4}$$

where $\sigma_\rho = \rho/\rho_{SL}$, $k_4 = k_1\rho_{SL} = \dfrac{\sigma\, C_{d_o}}{8}\rho_{SL}\pi R^2(\Omega R)^3$, and $k_5 = k_3\rho_{SL} = \dfrac{f\rho_{SL}}{2}$

2.1 Forward Flight

Ref. 5 shows that momentum theory gives

$$T = \rho\sqrt{V^2 + v^2}\,\pi R^2 2v \tag{5}$$

Assuming $V >> v$ gives

$$v = \frac{T}{2\rho\pi R^2 V} = k_6 \frac{T}{\rho}\frac{1}{V} \tag{6}$$

where $k_6 = 1/(2\pi R^2)$. Equation (6) is of the same form as the momentum theory solution for the induced velocity of a fixed-wing aircraft having an ideal wing of span $2R$ with an elliptical lift distribution.

Substituting equation (6) in (4)

$$\frac{P_{mr}}{\sigma_\rho} = \frac{T}{\sigma_\rho}\left(\frac{T}{\rho}\frac{k_6}{V}\right) + k_4\left(1 + k_2 V^2\right) + k_5 V^3$$

Multiplying by ρ_{SL}/ρ_{SL}

$$\frac{P_{mr}}{\sigma_\rho} = \frac{T}{\sigma_\rho}\left(\frac{T}{\rho/\rho_{SL}}\right)\frac{k_6}{\rho_{SL} V} + k_4\left(1 + k_2 V^2\right) + k_5 V^3$$

or

$$\frac{P_{mr}}{\sigma_\rho} = \left(\frac{T}{\sigma_\rho}\right)^2 \frac{k_7}{V} + k_4\left(1 + k_2 V^2\right) + k_5 V^3$$

where $k_7 = \dfrac{k_6}{\rho_{SL}} = \dfrac{1}{2\rho_{SL}\pi R^2}$

or, for a given airspeed, assuming $T \approx$ lift = W, where W is the aircraft weight

$$\frac{P_{mr}}{\sigma_\rho} = k_8\left(\frac{W}{\sigma_\rho}\right)^2 + k_9 \tag{7}$$

where $k_8 = \dfrac{k_7}{V} = \dfrac{1}{2\rho_{SL}\pi R^2 V}$ and $k_9 = k_4\left(1 + k_2 V^2\right) + k_5 V^3$

It should be noted that this equation is of the same form as that used to show the relationship between referred power (P/σ_ρ) and W/σ_ρ in Refs 3 and 4. The major assumption made when determining the induced velocity is that the forward airspeed is much greater than the induced velocity. However, a typical SHOL may have relative airspeeds approaching zero, thus negating the assumption. Solving equation (5) gives

$$v = \left(-\frac{V^2}{2} + \sqrt{\left(\frac{V^2}{2}\right)^2 + v_h^4}\right)^{1/2}$$

where v_h is the induced velocity at hover, given by

$$v_h = \sqrt{\frac{T}{2\rho\pi R^2}} = \sqrt{k_6\frac{T}{\rho}} = \sqrt{k_7\frac{T}{\sigma_\rho}} \tag{8}$$

Thus

$$v = \left(-\frac{V^2}{2} + \sqrt{\left(\frac{V^2}{2}\right)^2 + k_6^2\left(\frac{T}{\rho}\right)^2}\right)^{1/2} = \left(-\frac{V^2}{2} + \sqrt{\left(\frac{V^2}{2}\right)^2 + k_7^2\left(\frac{T}{\sigma_\rho}\right)^2}\right)^{1/2} \tag{9}$$

Quantities representing a hypothetical helicopter of conventional main and tail rotor configuration are given in Appendix A. These quantities have been substituted into the equations for induced velocity (6 & 9) to illustrate the validity of the induced velocity approximation in forward flight. This comparison is given in Appendix B and suggests that the relationship between P_{mr}/σ_ρ and W/σ_ρ given in equation (7) will only be valid for airspeeds above about 30 kn.

The induced velocity given by equation(9) is used to derive a relationship valid for all airspeeds. Substituting equation (9) into (4)

$$\frac{P_{mr}}{\sigma_\rho} = \frac{T}{\sigma_\rho}\left\{\left(-\frac{V^2}{2} + \sqrt{\left(\frac{V^2}{2}\right)^2 + k_7^2\left(\frac{T}{\sigma_\rho}\right)^2}\right)^{1/2}\right\} + k_4\left(1 + k_2 V^2\right) + k_5 V^3$$

or, with $T \approx W$

$$\frac{P_{mr}}{\sigma_\rho} = \frac{W}{\sigma_\rho}\left\{\left(-\frac{V^2}{2} + \sqrt{\left(\frac{V^2}{2}\right)^2 + k_7^2\left(\frac{W}{\sigma_\rho}\right)^2}\right)^{1/2}\right\} + k_9 \tag{10}$$

Thus for a given referred weight (W/σ_ρ) and airspeed (V), P_{mr}/σ_ρ and hence the referred power (P/σ_ρ) will be constant.

2.2 Hovering

For a hovering helicopter, $V = 0$, and substituting into equation (10)

$$\frac{P_{mr}}{\sigma_\rho} = \frac{W}{\sigma_\rho}\left(\sqrt{k_7}\sqrt{\frac{W}{\sigma_\rho}}\right) + k_4\left(1 + k_2(0)^2\right) + k_5(0)^3$$

$$= k_4 + \sqrt{k_7}\left(\frac{W}{\sigma_\rho}\right)^{3/2}$$

or

$$\frac{P_{mr}}{\sigma_\rho} = k_4 + k_{10}\left(\frac{W}{\sigma_\rho}\right)^{3/2} \tag{11}$$

where $k_{10} = \sqrt{k_7} = 1/\sqrt{2\rho_{SL}\pi R^2}$

2.3 Discussion

Figure 1 shows the relationship between P/σ_ρ and W/σ_ρ ($\approx T/\sigma_\rho$) at hover and for a forward speed of 35 kn. The plots were generated using equations (7), (10), and (11) for a hypothetical helicopter with characteristics given in Appendix A. It can be seen that for a given W/σ_ρ and V, P/σ_ρ is constant. Thus, by maintaining the W/σ_ρ ratio when attempting to determine the referred power margin for a given relative wind under widely varying atmospheric conditions, the P/σ_ρ ratio will be constant. It should be noted that the P/σ_ρ ratio will be the power required by the aircraft for the standard atmospheric conditions and does not indicate the power required for the atmospheric conditions encountered during a particular test, or whether that power is available if either the atmospheric conditions limit the engines or gearbox torque limits apply. This is discussed further in Section 4, using results obtained specifically for the Seahawk.

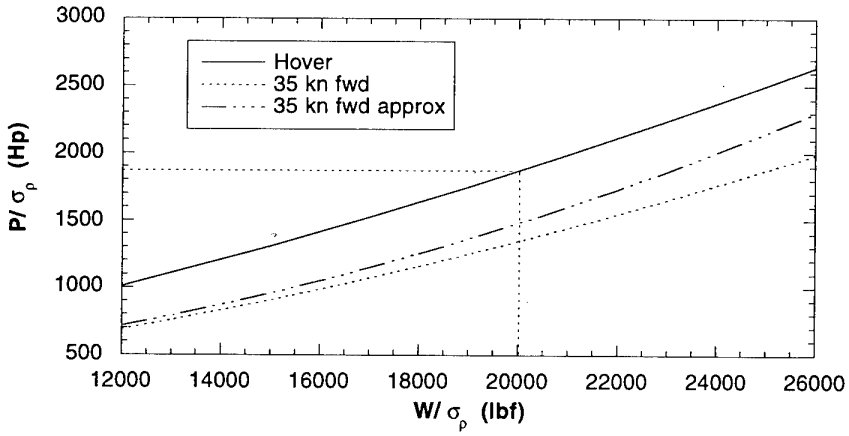

Figure 1. Relationship Between Referred Power (P/σ_ρ) and Referred Weight (W/σ_ρ)

It should also be noted that, in order to derive the relationships between P/σ_ρ and W/σ_ρ given here, a number of simplifications and assumptions were made that are discussed below.

1. Momentum theory is used to calculate the induced velocity which assumes that the inflow is uniform over the rotor disc. In reality, the induced velocity distribution over the disc is non-uniform and results in higher induced power requirements. Refs 12 and 13 suggest that the induced power requirements in hover may be underestimated by as much as 20%.
2. The calculation of the profile drag on the blades assumes no compressibility, stall, or reverse flow, and uses a mean drag coefficient with no allowance for variation with blade angle of attack. All these factors influence the profile drag to varying degrees depending on the flight condition.
3. The rotor blades are assumed to be rigid, but in reality a rotor blade twists and bends in complex varying modes as it rotates in azimuth.
4. The rotor blade is assumed to generate lift from the centre of rotation to the tip of the blade. In reality, the blade will generate lift outboard from the centre (from where the blade takes the shape of a lifting surface after the root cut-out) and a loss of lift occurs at the tip due to three-dimensional flow effects.
5. The rotor blade chord is assumed constant, although some blades have varying chord over the radius and some blades have unusual tip geometries. For example, the Lynx has a British Experimental Rotor Program tip and the S-70 family has a swept tip.
6. No vortex interaction effects are allowed for. In reality, the main rotor vortex may interact with the tail rotor and fuselage to produce unusual power requirements due to extra drag or a change in the angle of attack. Also, individual vortices being shed by one blade may have a significant effect on the angle of attack of the following blade.
7. Ground effect has not been accounted for, nor the effect of airwake induced by the superstructure of a ship. Ground effect reduces power requirements and the airwake would be expected to produce unusual power requirements due to extra drag or a change in angle of attack.

8. The fuselage drag is assumed to be independent of angle of attack and sideslip. In reality, the fuselage angle of attack will change with forward airspeed, thus changing the drag. The increase in fuselage drag (and thus power requirements) in side winds has not been considered here.
9. The main rotor thrust is assumed to be approximately equal to the aircraft weight. Ground effect and fuselage drag result in differences between the thrust and the weight.

The cumulative effect of the simplifications and assumptions made would be expected to result in variations between the theoretical and measured values of power required. In order to quantify the variation of P/σ_ρ for a given W/σ_ρ over a wide range of atmospheric conditions, program *GenHel* was used. *GenHel* accounts for many of the simplifications made in Sections 2.1 and 2.2 and has been shown to give good predictions of the flight dynamic behaviour of the S70 family of helicopters. The results for *GenHel* are given in Section 4.

3. TAIL ROTOR CONTROL

The tail rotor thrust is related to the main rotor power by

$$P_{mr} = Q_{mr}\Omega = T_{tr}l_{tr}\Omega$$

where Q_{mr} is the main rotor torque, T_{tr} is the tail rotor thrust, and l_{tr} is the distance from the main rotor centre of rotation to the tail rotor centre of thrust. Thus, for a given rotor speed, dividing by σ_ρ gives

$$\frac{P_{mr}}{\sigma_\rho} = k_{11}\frac{T_{tr}}{\sigma_\rho} \tag{12}$$

where $k_{11} = l_{tr}\Omega$

Thus, for a given P_{mr}/σ_ρ (and thus P/σ_ρ), T_{tr}/σ_ρ will be constant. Therefore, following from equation (10), for a given W/σ_ρ, T_{tr}/σ_ρ will be constant.

All parameters within Section 3, from this point onwards, will refer to the tail rotor unless otherwise stated, e.g. C_T refers to the thrust coefficient of the tail rotor rather than the main rotor.

Assuming the simplest case of a tail rotor with no pitch-flap coupling, the thrust of the tail rotor is given by Ref. 5 to be

$$\frac{C_T}{\sigma} = \frac{a}{4}\left[\left(\tfrac{2}{3}+\mu^2\right)\theta_o + \left(\tfrac{1}{2}+\tfrac{\mu^2}{2}\right)\theta_1 + \lambda\right] \tag{13}$$

where a is the blade lift curve slope, θ_o is the blade root collective pitch, θ_1 is the blade linear twist, and λ is the inflow ratio. The inflow ratio is given by $\lambda = (V\sin\alpha - v)/\Omega R$.

Three cases will be considered; forward flight, pure sidewards flight, and hovering.

3.1 Forward Flight

For forward flight, $\alpha = 0°$,

$$\mu = \frac{V\cos\alpha}{\Omega R} = \frac{V}{\Omega R}$$

$$\lambda = \frac{V\sin\alpha - v}{\Omega R} = \frac{-v}{\Omega R} = \frac{-k_6}{\Omega R V}\frac{T}{\rho} \text{ for } V > \sim 30 \text{ kn}$$

Equation (13) becomes

$$\frac{C_T}{\sigma} = \frac{a}{4}\left[\left(\tfrac{2}{3}+\mu^2\right)\theta_o + \left(\tfrac{1}{2}+\tfrac{\mu^2}{2}\right)\theta_1 - \frac{k_6}{\Omega R V}\frac{T}{\rho}\right]$$

Rearranging gives

$$\theta_o = \frac{1}{\tfrac{2}{3}+\mu^2}\left[\frac{4C_T}{\sigma a} + \frac{k_6}{\Omega R V}\frac{T}{\rho} - \frac{\theta_1}{2}\left(1+\mu^2\right)\right]$$

$$= \frac{1}{\tfrac{2}{3}+\mu^2}\left[\frac{4}{\sigma a}\frac{1}{\rho_{SL}\pi R^2(\Omega R)^2}\frac{T}{\rho/\rho_{SL}} + \frac{1}{2\rho_{SL}\pi R^2\Omega R V}\frac{T}{\rho/\rho_{SL}} - \frac{\theta_1}{2}\left(1+\mu^2\right)\right]$$

$$= \frac{1}{\left(\tfrac{2}{3}+\mu^2\right)\rho_{SL}\pi R^2}\left(\frac{4}{\sigma a}\frac{1}{(\Omega R)^2} + \frac{1}{2\Omega R V}\right)\frac{T}{\sigma_\rho} + \frac{\mu^2-1}{\tfrac{2}{3}+\mu^2}\left(\frac{\theta_1}{2}\right)$$

or, for a given airspeed

$$\theta_o = k_{12}\frac{T}{\sigma_\rho} + k_{13} \tag{14}$$

where $k_{12} = \dfrac{1}{\left(\frac{2}{3}+\mu^2\right)\rho_{SL}\pi R^2}\left(\dfrac{4}{\sigma a}\dfrac{1}{(\Omega R)^2} + \dfrac{1}{2\Omega R V}\right)$ and $k_{13} = \left(\dfrac{\mu^2-1}{\frac{2}{3}+\mu^2}\right)\dfrac{\theta_1}{2}$

However, as shown in Section 2.1, for V< ~30 kn, the approximation for v (and thus λ) is invalid. Using the solution for v from equation (9) gives

$$\lambda = \frac{-1}{\Omega R}\left(-\frac{V^2}{2} + \sqrt{\left(\frac{V^2}{2}\right)^2 + k_7^2\left(\frac{T}{\sigma_\rho}\right)^2}\right)^{1/2}$$

Equation (14) becomes

$$\frac{C_T}{\sigma} = \frac{a}{4}\left[\left(\frac{2}{3}+\mu^2\right)\theta_o + \left(\frac{1}{2}+\frac{\mu^2}{2}\right)\theta_1 - \frac{1}{\Omega R}\left(-\frac{V^2}{2} + \sqrt{\left(\frac{V^2}{2}\right)^2 + k_7^2\left(\frac{T}{\sigma_\rho}\right)^2}\right)^{1/2}\right]$$

Rearranging gives

$$\theta_o = \frac{1}{\frac{2}{3}+\mu^2}\left[\frac{4C_T}{\sigma a} + \frac{1}{\Omega R}\left(-\frac{V^2}{2} + \sqrt{\left(\frac{V^2}{2}\right)^2 + k_7^2\left(\frac{T}{\sigma_\rho}\right)^2}\right)^{1/2} - \frac{\theta_1}{2}\left(1+\mu^2\right)\right]$$

$$= \frac{1}{\frac{2}{3}+\mu^2}\left[\frac{4}{\sigma a}\frac{1}{\rho_{SL}\pi R^2(\Omega R)^2}\frac{T}{\sigma_\rho} + \frac{1}{\Omega R}\left(-\frac{V^2}{2} + \sqrt{\left(\frac{V^2}{2}\right)^2 + k_7^2\left(\frac{T}{\sigma_\rho}\right)^2}\right)^{1/2} - \frac{\theta_1}{2}\left(1+\mu^2\right)\right]$$

or, for a given airspeed

$$\theta_o = k_{14}\frac{T}{\sigma_\rho} + k_{15}\left(-\frac{V^2}{2} + \sqrt{\left(\frac{V^2}{2}\right)^2 + k_7^2\left(\frac{T}{\sigma_\rho}\right)^2}\right)^{1/2} + k_{13} \tag{15}$$

where $k_{14} = \dfrac{1}{\left(\frac{2}{3}+\mu^2\right)\rho_{SL}\pi R^2}\left(\dfrac{4}{\sigma a}\dfrac{1}{(\Omega R)^2}\right)$ and $k_{15} = \left(\dfrac{1}{\frac{2}{3}+\mu^2}\right)\dfrac{1}{\Omega R}$

Thus, for a given forward airspeed, θ_o is only a function of T/σ_ρ, and thus W/σ_ρ.

3.2 Sidewards Flight

For sidewards flight, α = ±90°, with flight to port corresponding to +90° and flight to starboard corresponding to -90°.

$$\mu = \frac{V\cos\alpha}{\Omega R} = 0$$

$$\lambda = \frac{V\sin\alpha - v}{\Omega R} = \frac{\pm V - v}{\Omega R}$$

Using the solution for v from equation (9), equation (13) becomes

$$\frac{C_T}{\sigma} = \frac{a}{4}\left[\left(\tfrac{2}{3}\right)\theta_o + \left(\tfrac{1}{2}\right)\theta_1 + \frac{1}{\Omega R}\left\{\pm V - \left(-\frac{V^2}{2} + \sqrt{\left(\frac{V^2}{2}\right)^2 + k_7^2\left(\frac{T}{\sigma_\rho}\right)^2}\right)^{1/2}\right\}\right]$$

Rearranging gives

$$\theta_o = \frac{3}{2}\left[\frac{4}{\sigma a}\frac{1}{\rho_{SL}\pi R^2(\Omega R)^2}\frac{T}{\rho/\rho_{SL}} - \frac{1}{\Omega R}\left\{\pm V - \left(-\frac{V^2}{2} + \sqrt{\left(\frac{V^2}{2}\right)^2 + k_7^2\left(\frac{T}{\sigma_\rho}\right)^2}\right)^{1/2}\right\} - \frac{\theta_1}{2}\right]$$

$$= \frac{6}{\sigma a}\frac{1}{\rho_{SL}\pi R^2(\Omega R)^2}\frac{T}{\sigma_\rho} - \frac{3}{2\Omega R}\left\{\pm V - \left(-\frac{V^2}{2} + \sqrt{\left(\frac{V^2}{2}\right)^2 + k_7^2\left(\frac{T}{\sigma_\rho}\right)^2}\right)^{1/2}\right\} - \frac{3\theta_1}{4}$$

or

$$\theta_o = k_{16}\frac{T}{\sigma_\rho} + k_{17}\left\{\pm V - \left(-\frac{V^2}{2} + \sqrt{\left(\frac{V^2}{2}\right)^2 + k_7^2\left(\frac{T}{\sigma_\rho}\right)^2}\right)^{1/2}\right\} + k_{18} \qquad (16)$$

where $k_{16} = \frac{6}{\sigma a}\frac{1}{\rho_{SL}\pi R^2(\Omega R)^2}$, $k_{17} = \frac{-3}{2\Omega R}$, and $k_{18} = \frac{-3\theta_1}{4}$

Thus for a given sidewards airspeed, θ_o is only a function of T/σ_ρ, and thus W/σ_ρ.

3.3 Hovering

For a hovering helicopter, $V = 0$,

$$\mu = \frac{V\cos\alpha}{\Omega R} = 0$$

$$\lambda = \frac{V\sin\alpha - v}{\Omega R} = \frac{-v}{\Omega R} = \frac{-\sqrt{k_7}}{\Omega R}\sqrt{\frac{T}{\sigma_\rho}}$$

Equation (13) becomes

$$\frac{C_T}{\sigma} = \frac{a}{4}\left[\left(\tfrac{2}{3}\right)\theta_o + \left(\tfrac{1}{2}\right)\theta_1 - \frac{\sqrt{k_7}}{\Omega R}\sqrt{\frac{T}{\sigma_\rho}}\right]$$

Rearranging gives

$$\theta_o = \frac{3}{2}\left[\frac{4C_T}{\sigma a} + \frac{\sqrt{k_7}}{\Omega R}\sqrt{\frac{T}{\sigma_\rho}} - \frac{\theta_1}{2}\right]$$

$$= \frac{3}{2}\left[\frac{4}{\sigma a}\frac{1}{\pi R^2(\Omega R)^2}\frac{T}{\rho} + \frac{\sqrt{k_7}}{\Omega R}\sqrt{\frac{T}{\sigma_\rho}} - \frac{\theta_1}{2}\right]$$

$$\theta_o = \frac{3}{2}\left[\frac{4}{\sigma a}\frac{1}{\rho_{SL}\pi R^2(\Omega R)^2}\frac{T}{\rho/\rho_{SL}} + \frac{\sqrt{k_7}}{\Omega R}\sqrt{\frac{T}{\sigma_\rho}} - \frac{\theta_1}{2}\right]$$

or

$$\theta_o = k_{16}\frac{T}{\sigma_\rho} + k_{19}\sqrt{\frac{T}{\sigma_\rho}} + k_{18} \tag{17}$$

where $k_{19} = \frac{3}{2}\frac{\sqrt{k_7}}{\Omega R} = \frac{3}{2\sqrt{2\rho_{SL}\pi R^2(\Omega R)^2}}$

Thus in hover, θ_o is only a function of T/σ_ρ, and thus W/σ_ρ.

3.4 Discussion

In order to illustrate the relationship between θ_o and W/σ_ρ, the data for the hypothetical helicopter of Appendix A were substituted into equations (14), (15), (16), and (17), and T_{tr}/σ_ρ was obtained using equation (12) for a given P_{mr}/σ_ρ (determined from a given W/σ_ρ). Figure 2 shows the relationship between θ_o and W/σ_ρ for each of the conditions considered above and confirms that θ_o is a function of W/σ_ρ for a range of flight conditions. Thus when attempting to determine the control margin under widely varying atmospheric conditions, θ_o will be constant for a given relative wind if the W/σ_ρ ratio is maintained.

As for the referred power required, similar simplifications and assumptions have been made. The cumulative effect of the simplifications and assumptions made would be expected to result in variations between the theoretical and measured values of blade angles. In order to quantify the variation of blade angles for a given W/σ_ρ over a wide range of atmospheric conditions, program *GenHel* was used. *GenHel* accounts for many of the simplifications made in Sections 3.1 to 3.3 and has been shown to give satisfactory predictions of the flight dynamic behaviour of the S70 family of helicopters.

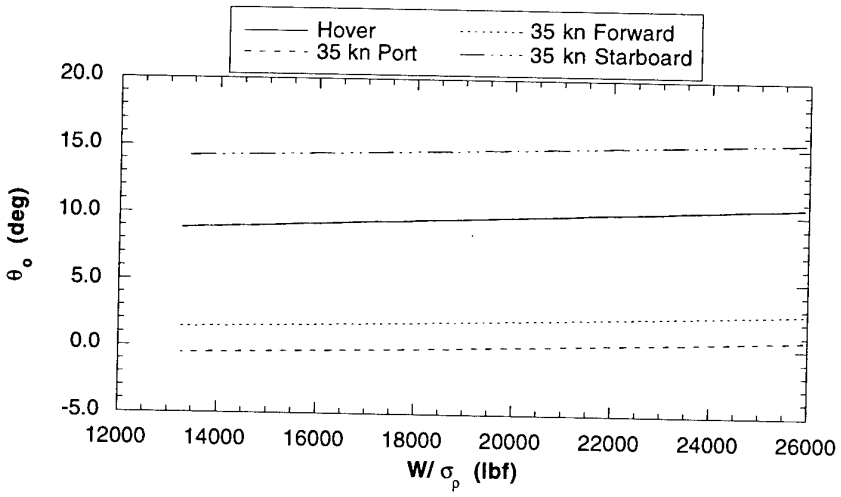

Figure 2. Variation of Tail Rotor Pitch (θ_o) with Referred Weight (W/σ_ρ)

4. GENHEL PREDICTIONS

Program *GenHel* was originally developed by Sikorsky for the US Army and has since been improved by NASA Ames (Refs 6 - 8). The code was specifically tailored for the S-70A Black Hawk and has since been modified for the S-70B Seahawk. Many of the simplifications and assumptions used for the equations developed in the preceding sections have been addressed in the aerodynamic representation in *GenHel*, as discussed below.

1. Blade element momentum theory is used to determine the induced velocity, with adjustments made to the induced velocity distribution over the rotor disk with forward speed. The result is a more accurate calculation of the induced power requirements.
2. The profile drag is calculated by first determining the local velocity and angle of attack at each blade element, then referring to wind tunnel data for the SC1095 aerofoil, as used by the S70 family of helicopters, to determine the segment lift and drag. The total profile drag is then determined by summing the drag at each blade element. This method is more accurate than assuming a mean drag coefficient and also allows for compressibility, stall, and reverse flow effects.
3. The main rotor is modelled as having the same geometry and preformed twist (non-linear) as the S70 and includes an empirically based allowance for dynamic twist.
4. Allowances are made for the main rotor downwash interacting with the fuselage, empennage, and tail rotor, but no allowance is made for the tail rotor interacting with the main rotor. Note that the modelled interaction effects are averaged, i.e. no account is made for local effects. Also, fin blockage effects are allowed for when determining the tail rotor thrust.
5. Fuselage and empennage aerodynamics are based on wind tunnel data, but results for rearward or sidewards flight at high velocities should be treated with caution.

In addition, the engines and flight control systems of the S-70B are well modelled to give accurate estimates of the torque and pilot control positions (Ref. 9).

Atmospheric relationships for both ISA and ISA+5°C are given in Appendix C, and Appendix D outlines the steps required to generate some of the input data for *GenHel*. To

define the atmospheric conditions, *GenHel* requires inputs of pressure altitude and density altitude to then calculate ambient density, pressure, temperature, and speed of sound (a_s).[1] The equivalent airspeed (V_{eq}) is also input, from which the true airspeed (V) is determined. *GenHel* does not currently have the capability of inputting ambient winds in the non-real time environment, but for trimming purposes, the aircraft may be trimmed at a given airspeed in the equivalent direction using parameter GAMHIC, which is the initial horizontal flight path angle. For example, trimming the aircraft at 35 kn, GAMHIC = 90° corresponds to trimming the aircraft in hover (with respect to the earth) in a 35 kn wind from starboard. The final variable input to *GenHel* was the aircraft weight.

In a typical FOCFT, a number of critical aircraft parameters are measured, all of which may be output from *GenHel*. For each run of *GenHel*, these outputs were:

1) Aircraft roll attitude
2) Pilot primary controls (longitudinal and lateral cyclic, collective, and pedals)
3) Main and tail rotor blade angles
4) Total torque (Q) and $Q/(\sigma_\rho)_{ISA+5}$

Note that the total torque is directly proportional to the total power, i.e. the relationships previously determined between W/σ_ρ and P/σ_ρ apply equally to $W/(\sigma_\rho)_{ISA+5}$ and $Q/(\sigma_\rho)_{ISA+5}$.

4.1 Effect of Density

To illustrate the effect on critical parameters due to variation in density, a range of atmospheric conditions was considered (Table 1). Ref. 1 suggested a range of pressures (28.0 inHg to 31.5 inHg) and temperatures (0°C to 50°C) that were used as the basis for Cases 1, 2, 4, and 6. Standard sea level conditions for an ISA+5°C atmosphere were used as a baseline for Case 3. In addition to these atmospheric conditions, a survey of the sea level conditions likely to be encountered in the Indian and Pacific Oceans was conducted (Appendix E). This survey suggested that the range of pressures given in Ref. 1 was realistic, although the range in temperature conditions would more likely be from -5°C to 40°C. The atmospheric pressure in the survey that corresponded to -5 °C was used as the basis for Case 5. The cases given in Table 1 were numbered in order of increasing density.

Table 1. Matrix of Ambient Conditions with Varying Density

Case	T_a (°C)	P_a (inHg)	h_p (ft)	ρ (slug/ft^3)	σ_ρ	$(\sigma_\rho)_{ISA+5}$	h_d (ft)	a_s (ft/s)
1	50	28.0	1824	0.0019836	0.83450	0.84900	6053	1182.3
2	50	31.5	-1431	0.0022314	0.93877	0.95506	2144	1182.3
3	20	29.9	0	0.0023364	0.98294	1.00000	587	1126.1
4	0	28.0	1824	0.0023465	0.98717	1.00430	440	1087.0
5	-5	28.6	1243	0.0024416	1.02718	1.04500	-919	1077.0
6	0	31.5	-1431	0.0026400	1.11060	1.12990	-3631	1087.0

For each case in Table 1, *GenHel* was run for hover and a relative wind of 35 kn true airspeed from ahead, port, and starboard for two referred weights of 15000 lbf and 20000 lbf. Table 2 summarises the equivalent airspeed (V_{eq}) and the actual weight that is input to *GenHel* for each of the cases.

[1] The speed of sound is used to determine compressibility effects on the main rotor.

Table 2. Equivalent Airspeed and Actual Weights

Case	σ_ρ	$(\sigma_\rho)_{ISA+5}$	V_{eq} (kn) [V = 35 kn]	W (lbf) $\left[\frac{W}{(\sigma_\rho)_{ISA+5}} = 15000 \text{ lbf}\right]$	W (lbf) $\left[\frac{W}{(\sigma_\rho)_{ISA+5}} = 20000 \text{ lbf}\right]$
1	0.83450	0.84900	32.0	12735	16980
2	0.93877	0.95506	33.9	14326	19101
3	0.98294	1.00000	34.7	15000	20000
4	0.98717	1.00430	34.8	15065	20086
5	1.02718	1.04500	35.5	15675	20900
6	1.11060	1.12990	36.9	16949	22598

It may be seen from Tables 3 and 4 that for a given relative wind and referred weight, the control positions, roll attitude, blade angles, and $Q/(\sigma_\rho)_{ISA+5}$ are almost a constant value. However, referring to the hover cases in Table 4, it should be noted that, although $Q/(\sigma_\rho)_{ISA+5}$ is about 94 %, the actual torque for Case 6 (105.8 %) is approaching the maximum continuous torque of 106 %, as illustrated in Figure 3. Thus, as noted in Section 2.3, although $Q/(\sigma_\rho)_{ISA+5}$ is well below torque limits, the actual power required is approaching those limits. In addition, there is no indication as to whether the engines are capable of producing this torque at those conditions.

Table 3. Critical Parameters over a Range of $(\sigma_\rho)_{ISA+5}$ for $W/(\sigma_\rho)_{ISA+5}$ of 15000 lbf

	Case	$(\sigma_\rho)_{ISA+5}$	ϕ (deg)	Long Cyc (%)	Lat Cyc (%)	Coll (%)	Ped (%)	A_{1s} (deg)	B_{1s} (deg)	$(\theta_0)_{mr}$ (deg)	$(\theta_0)_{tr}$ (deg)	Q (%)	$\frac{Q}{(\sigma_\rho)_{ISA+5}}$ (%)
Forward	1	0.84900	-1.3	53.6	46.3	39.9	61.5	-1.6	1.7	16.4	14.5	38.9	45.8
V=35 kn	2	0.95506	-1.3	53.4	46.2	40.7	61.7	-1.6	1.8	16.5	14.6	43.2	45.2
	3	1.00000	-1.3	53.1	46.1	40.7	61.5	-1.7	1.9	16.5	14.7	45.2	45.2
	4	1.00430	-1.3	53.1	46.1	40.5	61.2	-1.7	1.8	16.4	14.7	45.5	45.3
	5	1.00450	-1.3	52.9	46.1	40.7	61.3	-1.7	1.9	16.5	14.7	47.3	45.2
	6	1.12990	-1.3	52.4	46.0	41.4	61.6	-1.7	2.1	16.6	14.8	50.7	44.9
Port	1	0.84900	-9.8	63.2	46.4	45.7	79.4	-1.7	0.4	17.3	11.5	44.2	52.1
V=35 kn	2	0.95506	-9.8	62.8	46.4	46.5	79.4	-1.8	0.6	17.4	11.6	49.3	51.6
	3	1.00000	-9.9	62.6	46.5	46.5	79.2	-1.8	0.6	17.4	11.6	51.5	51.5
	4	1.00430	-9.9	62.4	46.5	46.3	78.9	-1.7	0.6	17.3	11.7	51.8	51.6
	5	1.00450	-9.9	62.3	46.5	46.5	78.8	-1.7	0.7	17.4	11.7	53.8	51.5
	6	1.12990	-9.9	62.0	46.4	47.2	78.9	-1.8	0.8	17.5	11.8	57.9	51.2
Stbd	1	0.84900	5.5	41.4	60.3	41.6	24.9	0.6	2.6	16.6	23.0	44.0	51.8
V=35 kn	2	0.95506	5.6	41.1	60.0	42.3	25.0	0.5	2.8	16.7	23.1	48.9	51.2
	3	1.00000	5.6	40.9	59.8	42.3	24.7	0.5	2.8	16.7	23.1	51.1	51.1
	4	1.00430	5.6	40.8	59.6	42.0	24.4	0.5	2.8	16.7	24.4	51.5	51.3
	5	1.00450	5.6	40.7	59.5	42.3	24.4	0.4	2.9	16.7	23.2	53.4	51.2
	6	1.12990	5.7	40.5	59.3	42.9	24.6	0.4	3.0	16.8	23.3	57.4	50.8
Hover	1	0.84900	-3.0	54.8	54.0	55.4	50.5	-0.8	1.2	18.8	19.4	55.5	65.3
V=0 kn	2	0.95506	-2.9	54.5	53.8	56.1	50.6	-0.8	1.3	18.9	19.6	61.8	64.7
	3	1.00000	-2.9	54.3	53.6	56.1	50.3	-0.9	1.4	18.9	19.6	64.6	64.6
	4	1.00430	-2.9	54.2	53.6	55.9	50.1	-0.9	1.4	18.8	19.6	64.9	64.7
	5	1.00450	-2.9	54.2	53.4	56.1	50.0	-0.9	1.4	18.9	19.7	67.4	64.5
	6	1.12990	-2.8	54.0	53.2	56.8	50.1	-0.9	1.5	19.0	19.8	72.5	64.2

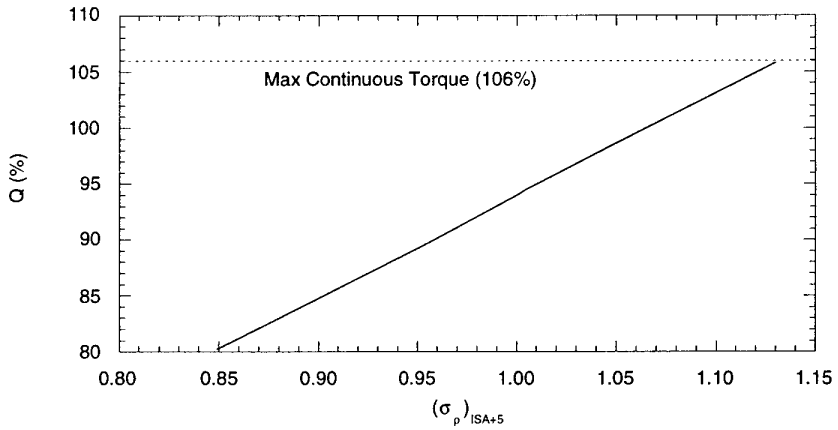

Figure 3. Variation of Q with $(\sigma_\rho)_{ISA+5}$ at Hover for $W/(\sigma_\rho)_{ISA+5}$ of 20000 lbf

Table 4. Critical Parameters over a Range of $(\sigma_\rho)_{ISA+5}$ for $W/(\sigma_\rho)_{ISA+5}$ of 20000 lbf

	Case	$(\sigma_\rho)_{ISA+5}$	ϕ (deg)	Long Cyc (%)	Lat Cyc (%)	Coll (%)	Ped (%)	A_{1s} (deg)	B_{1s} (deg)	$(\theta_0)_{mr}$ (deg)	$(\theta_0)_{tr}$ (deg)	Q (%)	$\frac{Q}{(\sigma_\rho)_{ISA+5}}$ (%)
Forward	1	0.84900	-1.4	51.8	45.6	54.7	59.6	-2.1	2.8	18.7	17.3	55.4	65.3
V=35 kn	2	0.95506	-1.4	51.5	45.4	55.7	59.8	-2.2	2.9	18.8	17.4	61.8	64.7
	3	1.00000	-1.4	51.2	45.2	55.7	59.6	-2.2	3.0	18.8	17.5	64.6	64.6
	4	1.00430	-1.4	51.1	45.1	55.3	59.2	-2.2	3.0	18.8	17.5	65.1	64.7
	5	1.04500	-1.4	50.8	45.0	55.7	59.2	-2.2	3.0	18.8	17.6	67.6	64.7
	6	1.12990	-1.4	50.4	44.9	56.6	59.5	-2.3	3.2	19.0	17.6	72.8	64.4
Port	1	0.84900	-8.3	63.7	44.2	59.4	70.9	-2.4	0.3	19.4	15.5	61.3	72.2
V=35 kn	2	0.95506	-8.3	63.5	44.0	60.4	70.9	-2.5	0.4	19.6	15.7	68.5	71.7
	3	1.00000	-8.3	63.3	44.0	60.4	70.5	-2.5	0.4	19.6	15.8	71.7	71.7
	4	1.00430	-8.3	63.1	44.0	60.0	70.1	-2.5	0.4	19.5	15.8	72.3	72.0
	5	1.04500	-8.3	63.0	43.9	60.4	70.0	-2.5	0.4	19.5	15.9	75.1	71.9
	6	1.12990	-8.3	62.9	43.8	61.3	70.2	-2.5	0.5	19.7	16.0	80.9	71.6
Stbd	1	0.84900	3.8	41.3	64.3	55.0	24.5	0.9	3.3	18.7	25.2	60.0	70.6
V=35 kn	2	0.95506	3.9	41.0	64.0	56.0	24.7	0.8	3.4	18.9	25.3	66.9	70.1
	3	1.00000	3.9	40.8	63.7	56.0	24.3	0.8	3.4	18.9	25.4	69.9	69.9
	4	1.00430	3.9	40.7	63.5	55.6	23.9	0.7	3.4	18.8	25.5	70.4	70.1
	5	1.04500	3.9	40.5	63.3	55.9	23.7	0.7	3.5	18.9	25.5	73.3	70.1
	6	1.12990	4.0	40.4	63.1	56.8	23.8	0.6	3.5	19.0	25.7	78.8	69.7
Hover	1	0.84900	-3.1	55.1	54.4	70.0	42.8	-1.1	1.2	21.1	23.5	80.2	94.5
V=0 kn	2	0.95506	-3.0	55.0	54.0	71.1	42.8	-1.2	1.3	21.2	23.7	89.7	93.9
	3	1.00000	-3.0	54.7	53.8	71.0	42.3	-1.2	1.3	21.2	23.8	94.0	94.0
	4	1.00430	-3.0	54.6	53.7	70.7	41.9	-1.2	1.3	21.2	23.8	94.5	94.1
	5	1.04500	-3.0	54.5	53.6	71.0	41.8	-1.2	1.3	21.2	23.9	98.2	94.0
	6	1.12990	-2.9	54.5	53.3	72.0	42.0	-1.3	1.4	21.4	24.0	105.8	93.6

Examination of Tables 3 and 4 indicates that, for the range of conditions considered, $Q/(\sigma_\rho)_{ISA+5}$ and the control positions are essentially constant for a given relative wind and $W/(\sigma_\rho)_{ISA+5}$.

4.2 Effect of Temperature

Since the speed of sound (a_s) at sea level is purely a function of temperature, a range of atmospheric conditions were considered where the temperature varied, but the density remained constant. These conditions would illustrate the significance of compressibility effects to critical parameters. Cases 3, 7, 8, and 9 all maintain the same density (0.0023364 slug/ft^3) over a temperature range from -5°C to 50 °C. The density altitude is therefore fixed at 587 ft and the equivalent airspeed of 34.7 kn corresponds with a true airspeed of 35 kn. A summary of the conditions considered is given in Table 5.

Table 5. Matrix of Ambient Conditions for $(\sigma_\rho)_{ISA+5}$ of 1

Case	T_a (°C)	P_a (inHg)	h_p (ft)	a_s (ft/s)
7	50	33.0	-2721	1182.3
3	20	29.9	0	1126.1
8	0	27.9	1942	1087.0
9	-5	27.4	2446	1077.0

It can be seen from Tables 6 and 7 that for a given relative wind and referred weight, temperature effects result in only small variations in power requirements and control positions that, upon comparison with Tables 4 and 5, are less than those through changes in density. Thus for the conditions considered, compressibility effects are negligible, i.e. $Q/(\sigma_\rho)_{ISA+5}$ and control positions are essentially constant for a given relative wind and $W/(\sigma_\rho)_{ISA+5}$.

Table 6. Critical Parameters over a Range of T_a for $(\sigma_\rho)_{ISA+5}$ of 1 and $W/(\sigma_\rho)_{ISA+5}$ of 15000 lbf

	Case	T_a (°C)	ϕ (deg)	Long Cyc (%)	Lat Cyc (%)	Coll (%)	Ped (%)	A_{1s} (deg)	B_{1s} (deg)	$(\theta_0)_{mr}$ (deg)	$(\theta_0)_{tr}$ (deg)	Q (%)	$\frac{Q}{(\sigma_\rho)_{ISA+5}}$ (%)
Forward	7	50	-1.3	53.2	46.2	41.0	61.9	-1.7	1.9	16.5	14.6	45.0	45.0
V=35 kn	3	20	-1.3	53.1	46.1	40.7	61.5	-1.7	1.9	16.5	14.7	45.2	45.2
	8	0	-1.3	53.1	46.1	40.5	61.2	-1.7	1.8	16.4	14.7	45.4	45.4
	9	-5	-1.3	53.1	46.1	40.4	61.1	-1.7	1.8	16.4	14.7	45.4	45.4
Port	7	50	-9.8	62.7	46.4	46.8	79.5	-1.8	0.6	17.4	11.6	51.3	51.3
V=35 kn	3	20	-9.9	62.6	46.5	46.5	79.2	-1.8	0.6	17.4	11.6	51.5	51.5
	8	0	-9.9	62.5	46.5	46.3	78.8	-1.7	0.6	17.3	11.7	51.7	51.7
	9	-5	-9.9	62.4	46.5	46.2	78.7	-1.7	0.6	17.3	11.7	51.7	51.7
Stbd	7	50	5.6	41.0	59.9	42.6	25.0	0.5	2.8	16.8	23.1	51.0	51.0
V=35 kn	3	20	5.6	40.9	59.8	42.3	24.7	0.5	2.8	16.7	23.1	51.1	51.1
	8	0	5.6	40.8	59.6	42.0	24.4	0.5	2.8	16.7	23.2	51.3	51.3
	9	-5	5.6	40.8	59.6	42.0	24.4	0.5	2.8	16.7	23.2	51.3	51.3
Hover	7	50	-2.9	54.5	53.7	56.4	50.6	-0.9	1.4	18.9	19.6	64.5	64.5
V=0 kn	3	20	-2.9	54.3	53.6	56.1	50.3	-0.9	1.4	18.9	19.6	64.6	64.6
	8	0	-2.9	54.3	53.6	55.9	50.1	-0.9	1.4	18.8	19.6	64.7	64.7
	9	-5	-2.9	54.2	53.6	55.8	50.0	-0.9	1.4	18.8	19.6	64.7	64.7

Table 7. Critical Parameters over a Range of T_a for $(\sigma_\rho)_{ISA+5}$ of 1 and $W/(\sigma_\rho)_{ISA+5}$ of 20000 lbf

	Case	T_a (°C)	ϕ (deg)	Long Cyc (%)	Lat Cyc (%)	Coll (%)	Ped (%)	A_{1s} (deg)	B_{1s} (deg)	$(\theta_0)_{mr}$ (deg)	$(\theta_0)_{tr}$ (deg)	Q (%)	$\frac{Q}{(\sigma_\rho)_{ISA+5}}$ (%)
Forward	7	50	-1.4	51.3	45.3	56.2	60.0	-2.2	3.0	18.9	17.5	64.5	64.5
V=35 kn	3	20	-1.4	51.2	45.2	55.7	59.6	-2.2	3.0	18.8	17.5	64.6	64.6
	8	0	-1.4	51.1	45.1	55.3	59.2	-2.2	2.9	18.8	17.5	64.9	64.9
	9	-5	-1.4	51.1	45.1	55.2	59.1	-2.2	2.9	18.7	17.5	64.9	64.9
Port	7	50	-8.3	63.5	44.0	60.9	71.0	-2.5	0.4	19.6	15.7	71.6	71.6
V=35 kn	3	20	-8.3	63.3	44.0	60.4	70.5	-2.5	0.4	19.6	15.8	71.7	71.7
	8	0	-8.3	63.1	44.0	60.0	70.0	-2.5	0.4	19.5	15.8	72.0	72.0
	9	-5	-8.3	63.1	44.0	59.9	69.9	-2.5	0.4	19.5	15.8	72.1	72.1
Stbd	7	50	3.9	41.0	63.8	56.5	24.7	0.8	3.4	18.9	25.4	69.9	69.9
V=35 kn	3	20	3.9	40.8	63.7	56.0	24.3	0.8	3.4	18.9	25.4	69.9	69.9
	8	0	3.9	40.7	63.5	55.6	23.9	0.7	3.4	18.8	25.4	70.2	70.2
	9	-5	3.9	40.6	63.5	55.5	23.8	0.7	3.4	18.8	25.5	70.3	70.3
Hover	7	50	-3.0	54.9	53.9	71.5	42.8	-1.2	1.3	21.3	23.7	93.7	93.7
V=0 kn	3	20	-3.0	54.7	53.8	71.0	42.3	-1.2	1.3	21.2	23.8	94.0	94.0
	8	0	-3.0	54.6	53.7	70.7	41.9	-1.2	1.3	21.2	23.8	94.1	94.1
	9	-5	-3.0	54.6	53.7	70.6	41.8	-1.2	1.3	21.1	23.8	94.2	94.2

5. CONCLUDING REMARKS

By making a series of assumptions and simplifications, it has been shown theoretically that, for a given referred weight and relative wind, the referred power requirements and control positions are constant. This relationship holds true regardless of the atmospheric conditions chosen for the reference, i.e. ISA or off-ISA conditions, and has been confirmed by using program *GenHel* over a wide range of atmospheric conditions, for two referred weights and with ISA+5°C as the reference. Although a small variation in the *GenHel* results is apparent at a given relative wind velocity and referred weight, the referred power requirements and control positions are essentially constant.

ACKNOWLEDGEMENT

The author would like to extend thanks and appreciation to LCDR M. Henschke for his willingness to clarify certain aspects of flight testing.

REFERENCES

1. Henschke, M., "S-70B-2/FFG-7 First of Class Flight Trial Report," RAN Aircraft Maintenance and Flight Trials Unit Report 3/94, RAN Air Station, Nowra, NSW, Australia, November 1995.

2. Henschke, M., "HMAS SUCCESS/SEA KING Mk 50/50A First of Class Flight Trial," RAN Aircraft Maintenance and Flight Trials Unit Report 1/92, RAN Air Station, Nowra, NSW, Australia, July 1993.

3. Daniels, S. A., "Explanation of RAN Aircraft Weight Corrections," RAN Aircraft Maintenance and Flight Trials Unit Report 5/88, RAN Air Station, Nowra, NSW, Australia, November 1988.

4. Vidmar, F., "Report on Power and Control Margins for Helicopter Flight in Ship Board Operations," Internal RAN Naval Aircraft Logistics Office Report, AMAFTU File AN739-41-001, RAN Air Station, Nowra, NSW, Australia, September 1989.

5. Prouty, R. W., *Helicopter Performance, Stability, and Control,* PWS Engineering, Boston, USA, 1986.

6. Howlett, J. J., "UH-60A Black Hawk Engineering Simulation Program: Volume I - Mathematical Model," NASA Contractor Report 166309, National Aeronautics and Space Administration, Ames Research Center, Moffett Field, California, USA, December 1981.

7. Howlett, J. J., "UH-60A Black Hawk Engineering Simulation Program: Volume II - Background Report," NASA Contractor Report 166310, National Aeronautics and Space Administration, Ames Research Center, Moffett Field, California, USA, December 1981.

8. Ballin, M. G., "Validation of a Real-Time Engineering Simulation of the UH-60A Helicopter," NASA Technical Memorandum 88360, National Aeronautics and Space Administration, Ames Research Center, Moffett Field, California, USA, 1987.

9. Arney, A. M. and Blackwell, J., " Australian Dynamic Testing of Sikorsky S-70B-2 Helicopters in Support of Operations from Ships," NCP 95/1, Proceedings of the 6th Australian Aeronautical Conference, Melbourne, 20-22 March 1995, Institution of Engineers, Australia, 1995.

10. Beck, C. P. and Funk Jr, J. D., " Development and Validation of a Seahawk Blade Element Model in Support of Rotorcraft Shipboard Operations," Proceedings of the Rotorcraft Simulation Conference, London, 18-19 May 1994, Royal Aeronautical Society, UK, 1994.

11. Layton, D. M., *Helicopter Performance,* Matrix Publishers, Inc., Beaverton, Oregon, USA 1984.

12. Reddy, K. R. and Gilbert, N. E., "Comparison with Flight Data of Hover Performance Using Various Rotor Wake Models," Proceedings of the 13th European Rotorcraft Forum, Arles, France, 8-11 September 1987, Paper 2-12, 1987.

13. Williams, M. J. and Arney, A. M., "Helicopter Hover Performance Estimation Comparison with UH-1H Iroquois Flight Data," ARL Aerodynamics TM 377, Defence Science and Technology Organisation, Department of Defence, Australia, April 1986.

14. Houghton, E. L. and Brock, A. E., *Aerodynamics For Engineering Students*, Butler & Tanner Ltd, Frome and London, Great Britain, 1980.

15. "U.S. Navy Marine Climatic Atlas of the World. Volume III. Indian Ocean," NAVAIR-50-1C-530, Naval Air Systems Command, Washington DC, USA, March 1976.

16. "U.S. Navy Marine Climatic Atlas of the World. Volume V. South Pacific Ocean," NAVAIR-50-1C-532-REV, Naval Air Systems Command, Washington DC, USA, October 1979.

17. Kreyszig, Erwin, *Advanced Engineering Mathematics, Fourth Edition,* John Wiley and Sons, Inc, NY, USA, 1979.

18. CDROM titled *US Navy Marine Climatic Atlas of the World, Version 1.1,* Fleet Numerical Meteorology and Oceanography Detachment, Asheville, NC, USA, August 1995.

19. "U.S. Navy Marine Climatic Atlas of the World. Volume I. North Atlantic Ocean," NAVAIR-50-1C-528, Naval Air Systems Command, Washington DC, USA, December 1974.

20. "U.S. Navy Marine Climatic Atlas of the World. Volume II. North Pacific Ocean," NAVAIR-50-1C-529, Naval Air Systems Command, Washington DC, USA, March 1977.

21. "U.S. Navy Marine Climatic Atlas of the World. Volume IV. South Atlantic Ocean," NAVAIR-50-1C-531, Naval Air Systems Command, Washington DC, USA, March 1978.

22. "U.S. Navy Marine Climatic Atlas of the World. Volume VI. Arctic Ocean," NAVWEPS-50-1C-533, Bureau of Naval Weapons, Washington DC, USA, February 1963.

23. "U.S. Navy Marine Climatic Atlas of the World. Volume VII. Antarctic Ocean," NAVAIR-50-1C-50, Bureau of Naval Weapons, Washington DC, USA, September 1965.

24. "U.S. Navy Marine Climatic Atlas of the World. Volume VIII. The World," NAVAIR-50-1C-54, Naval Air Systems Command, Washington DC, USA.

25. "U.S. Navy Marine Climatic Atlas of the World. Volume IX. World Wide Means and Standard Deviations," NAVAIR-50-1C-65, Naval Oceanography Command, Washington DC, USA, May 1981.

APPENDIX A - HYPOTHETICAL HELICOPTER CHARACTERISTICS

The quantities given below represent a hypothetical helicopter, in a similar class to the Black Hawk, that was used to generate the figures in Sections 2 and 3, as well as Appendix B, by using the equations developed in this document. The ISA sea-level density was used as the reference, i.e. ρ_o = 0.002377 slug/ft^3 (1.225 kg/m^3), although other atmospheric conditions (e.g. ISA+5°C) would give similar trends.

Fuselage Characterisitics: $f = 21.53$ ft^2, $l_{tr} = 32.81$ ft

Table A1. Main and Tail Rotor Characteristics

	b	c (ft)	R (ft)	σ	C_{d_o}	Ω (rad/s)	a (/rad)	θ_1 (deg)
MAIN ROTOR	4	1.64	26.25	0.07955	0.008	27	6	-8
TAIL ROTOR	4	0.82	4.92	0.21221	0.008	125	6	-8

Table A2. Main Rotor Constants

k_1 (ft^{5}rad^{3}s^{-3})	k_2 (ft^{-2}rad^{-2}s^2)	k_3 (ft^2)	k_4 (slug.ft^{2}rad^{3}s^{-3})	k_5 (slug.ft^{-1})	k_6 (ft^{-2})
6.1307E+7	8.5602E-6	1.0765E+1	1.4573E+5	2.5588E-2	2.3097E-4
k_7 (slug^{-1}ft^{-5})	k_8 (slug^{-1}ft^{-6}s)	k_9(hover) (slug.ft^{2}s^{-3})	k_9 (35 kn) (slug.ft^{2}s^{-3})	k_{10} (slug$^{1/2}$ft$^{-5/2}$)	k_{11} (ft.rad.s^{-1})
9.7170E-2	1.6449E-3	1.4573E+5	1.5536E+5	3.1172E-1	8.8587E+2

Table A3. Tail Rotor Constants

k_7 (slug^{-1}ft^{-5})	k_{12} (slug^{-1}ft^{-1}rad^{-1}s^2)	k_{13} (rad)	k_{14} (slug^{-1}ft^{-1}rad^{-1}s^2)	k_{15} (ft^{-1}rad^{-1}s)
2.7661	1.8063E-4	1.0234E-1	6.7985E-5	2.4057E-3
k_{16} (slug^{-1}ft^{-1}rad^{-1}s^2)	k_{17} (ft^{-1}rad^{-1}s)	k_{18} (rad)	k_{19} (slug$^{1/2}$ft$^{-7/2}$rad^{-1}s)	
6.8926E-5	-2.4390	1.0472E-1	4.0565E-3	

APPENDIX B - INDUCED VELOCITY RELATIONSHIPS

Figure B1 shows the variation of induced velocity with airspeed, comparing the results using the 'forward flight approximation' with those obtained solving the momentum theory equation. Ref. 5 suggests that the approximation gives essentially the same results for airspeeds above 30 kn (~ 50 ft/s). The results given here using the hypothetical helicopter show that the approximation gives reasonable results above 30 kn.

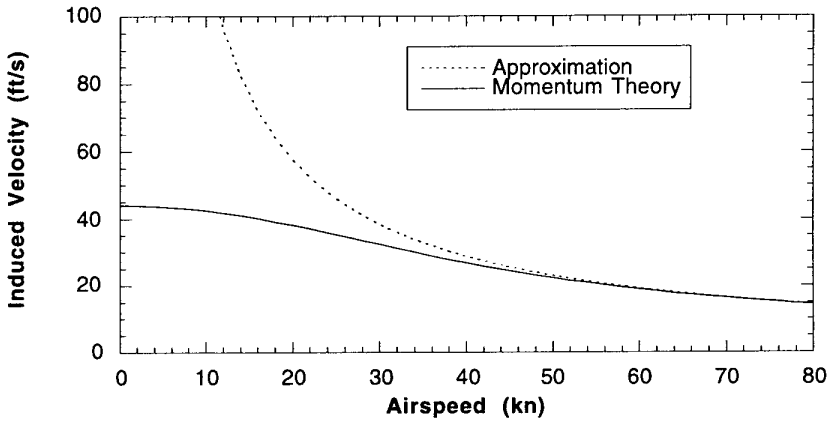

Figure B1. Variation of Induced Velocity with Airspeed for a Fixed W/σ_ρ (20000 lbf)

Figure B2 shows the variation of induced velocity with W/σ_ρ for a fixed airspeed, comparing the results using the 'forward flight approximation' with those obtained using momentum theory. It can be seen that the approximation gives results closer to the momentum theory results at lower W/σ_ρ, and that both methods give the same trends, i.e. induced velocity increases with W/σ_ρ.

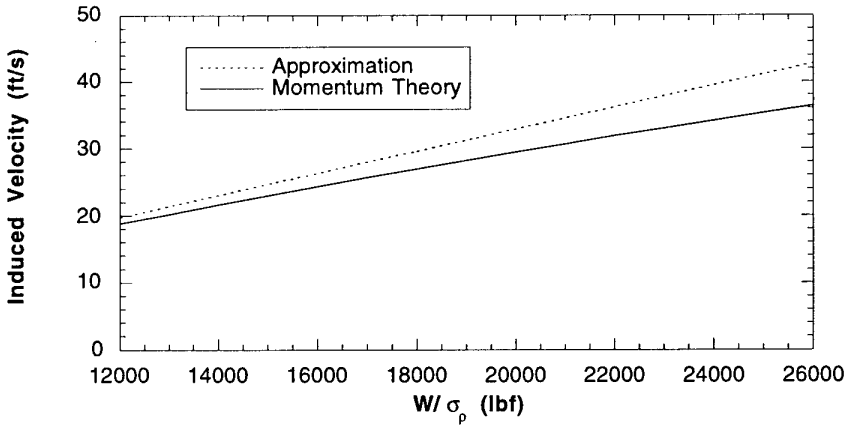

Figure B2. Variation of Induced Velocity with W/σ_ρ for a Fixed Airspeed (35 kn)

APPENDIX C - ATMOSPHERIC RELATIONSHIPS

C1. INTRODUCTION

SHOLs are usually developed for a range of operating weights, both day and night, for a defined standard atmosphere. If the actual atmospheric conditions on a given day are not identical to the atmospheric conditions for which the SHOLs were developed, weight corrections must be applied. The International Standard Atmosphere (ISA) is defined as having a temperature of 15°C (288.15 K), at sea-level. Applying weight corrections for any day with temperatures higher than 15°C is restrictive to the RAN, given that most flying in Australia's region is conducted in conditions warmer than ISA. By using an atmosphere based on ISA+5°C conditions, weight corrections need not be applied until the sea-level temperature rises above 20°C. AMAFTU have recently moved towards conducting FOCFTs under ISA+5°C conditions (Refs 1 and 2). This appendix examines the effect on the standard atmopsheric equations of changing the baseline atmosphere from ISA conditions to ISA+5°C conditions.

C2. DEFINITIONS

The International Standard Atmosphere (ISA) sea-level conditions are defined as ambient pressure of 101325 N/m^2 (1013.2 hPa or 29.92 inHg), ambient air density of 1.225 kg/m^3 (0.002377 slug/ft^3), and ambient air temperature of 15°C (288.15 K).

The pressure altimeter is a barometer that measures the ambient pressure of the aircraft under consideration but is graduated in feet and is calibrated for ISA conditions. If the actual mean sea-level (MSL) pressure, known as QNH, differs from the ISA MSL pressure (29.92 inHg),[1] there is a small subscale on the altimeter that allows QNH to be set. With QNH set in the subscale, the altimeter will read altitude (height above MSL).

Pressure Height (h_p) is the height in the International Standard Atmosphere above sea-level at which the ambient pressure equals that of the aircraft under consideration. With 29.92 inHg on the subscale, the altimeter reads pressure height.

Density Height (h_d) is the height in the International Standard Atmosphere that corresponds to the ambient air density of the aircraft under consideration.

C3. STANDARD ATMOSPHERIC EQUATIONS

C3.1 All Conditions

The equations in this section apply to both ISA and ISA+5°C conditions.

The ideal gas equation for a given altitude is

$$P_a = \rho R_g T_a \tag{C1}$$

where P_a is the ambient air pressure (N/m^2), ρ is the ambient air density (kg/m^3), R_g is the gas constant for air (287.05 Nm/kg.K), and T_a is the ambient air temperature (K).

Now,

$$\frac{(P_a)_1}{(P_a)_2} = \frac{\rho_1}{\rho_2}\frac{R_g}{R_g}\frac{(T_a)_1}{(T_a)_2} = \frac{\rho_1}{\rho_2}\frac{(T_a)_1}{(T_a)_2} \tag{C2}$$

where subscripts *1* and *2* denote two different altitudes or atmospheric conditions.

---

[1] The altimeter subscale on the S-70B-2 is graduated in units of inHg.

C3.2 ISA Conditions

The equations in this section only apply to ISA conditions, e.g. T_{SL} refers to 288.15 K.

The pressure, density, and temperature ratios are defined by

$$\delta = \frac{P_a}{P_{SL}},\ \theta = \frac{T_a}{T_{SL}},\ \text{and}\ \sigma_\rho = \frac{\rho}{\rho_{SL}}$$

where subscript *SL* denotes sea-level conditions.

Thus, from equation (C2),

$$\delta = \sigma_\rho \theta$$

which on rearranging gives

$$\sigma_\rho = \frac{\delta}{\theta} \tag{C3}$$

For the troposphere, i.e. altitude from sea-level up to 11000 m, (Ref. 14),

$$\delta = \theta^{\frac{g}{LR_g}} \tag{C4}$$

where L is the lapse rate (0.0065 K/m) and g is gravitational acceleration (9.80665 m/s^2).

Now,

$$T_a = T_{SL} - Lh$$

which on dividing by T_{SL} gives

$$\theta = 1 - \frac{L}{T_{SL}}h \tag{C5}$$

where h is the height (m) above sea-level.

Substituting for θ in equation (C4) gives

$$\delta = \left(1 - \frac{L}{T_{SL}}h\right)^{\frac{g}{LR_g}} \tag{C6}$$

As mentioned in Section C2, the aircraft altimeter indicates altitude, in units of ft, purely as a function of pressure and is calibrated for standard ISA conditions, i.e. P_{SL} is 101325 N/m^2 (29.92 inHg), ρ_{SL} is 1.225 kg/m^3 (0.002377 slug/ft^3), and T_{SL} is 15°C (288.15 K). By setting the altimeter subscale to ISA MSL pressure, the pressure altitude may be read directly from the altimeter. However, if the pressure ratio is to be determined directly from equation (C6) by substituting the pressure altitude h_p for h, the conversion from ft to m (1 ft = 0.3048 m) must be incorporated. Thus, equation (C6) becomes

$$\delta = \left[1 - \frac{0.0065}{288.15}\left(0.3048h_p\right)\right]^{\frac{9.80665}{0.0065\times 287.05}} = \left(1 - 6.8756\times 10^{-6}h_p\right)^{5.2559} \tag{C7}$$

Conversely, to determine the pressure altitude from the pressure ratio, equation (C7) may be rearranged to give

$$h_p = \left(1 - \delta^{\frac{1}{5.2559}}\right)\frac{1}{6.8756\times 10^{-6}} = 1.4544\times 10^5\left(1 - \delta^{0.19026}\right) \tag{C8}$$

Aircraft and engine performance are a function of air pressure, temperature, and density. The instruments to measure ambient pressue (altimeter) and outside air temperature (OAT gauge)

are a standard fit to aircraft and may be used to determine air density. On any given day, the pressure ratio for the aircraft under consideration may be determined by substituting the pressure altitude into equation (C7). The temperature ratio may be determined from the OAT. The ambient density may then be determined using equation (C3). A common method of displaying helicopter performance as a function of density is to plot torque required against density altitude. The density altitude (h_d) may be determined from the density ratio as follows:

Dividing equation (C4) by θ gives

$$\frac{\delta}{\theta} = \theta^{\frac{g}{LR_g}-1} \tag{C9}$$

Thus, from equations (C5) and (C9),

$$\sigma_\rho = \left(1 - \frac{L}{T_{SL}} h_d\right)^{\frac{g}{LR_g}-1} \tag{C10}$$

Rearranging equation (C10), the density altitude (in units of ft) is given by

$$h_d = \left(1 - \sigma_\rho^{\frac{LR_g}{g-LR_g}}\right)\frac{T_{SL}}{L} = \frac{1}{0.3048}\left(1 - \sigma_\rho^{\frac{0.0065\times 287.05}{9.80665-0.0065\times 287.05}}\right)\frac{288.15}{0.0065}$$

$$= 1.4544\times 10^5\left(1-\sigma_\rho^{0.235}\right) \tag{C11}$$

C3.3 ISA+5°C Conditions

The ISA+5°C sea-level conditions are defined as ambient pressure of 101325 N/m^2 (1013.2 hPa or 29.92 inHg), and ambient air temperature of 20°C (293.15 K). Using equation (C1), the sea-level density may be determined by

$$\rho_{SL.ISA+5} = \frac{P_{SL.ISA+5}}{R_g T_{SL.ISA+5}} = \frac{101325}{287.05\times 293.15} = 1.204 \text{ kg/m}^3 \text{ (0.002336 slug/ft}^3\text{)}$$

where subscript *ISA+5* denotes ISA+5°C conditions.

Since the MSL pressure for ISA and ISA+5°C are identical, and the pressure altimeter reads altitude purely as a function of pressure, the pressure ratio and pressure altitude may be determined directly from equations (C7) and (C8) for ISA+5°C conditions. However, the temperature ratio and thus density ratio for ISA+5°C will be quite different from ISA, i.e.

$$\delta_{ISA+5} = \frac{P_a}{P_{SL,ISA+5}} = \frac{P_a}{P_{SL}} = \delta$$

$$\theta_{ISA+5} = \frac{T_a}{T_{SL,ISA+5}} \text{ and } \left(\sigma_\rho\right)_{ISA+5} = \frac{\rho}{\rho_{SL,ISA+5}}$$

Since density altitude is defined as the height which corresponds to the ambient density for ISA conditions, the σ_ρ equivalent to $(\sigma_\rho)_{ISA+5}$ must be determined, so that equation (C11) may be used to determine density altitude.

The equivalent ISA density ratio may be determined from the ISA+5 density ratio as follows:

$$\sigma_\rho = \frac{\rho}{\rho_{SL}} \text{ and } (\sigma_\rho)_{ISA+5} = \frac{\rho}{\rho_{SL,ISA+5}}$$

which gives

$$\sigma_\rho = (\sigma_\rho)_{ISA+5} \frac{\rho_{SL,ISA+5}}{\rho_{SL}} \tag{C12}$$

Equation (C2) gives

$$\frac{P_{SL,ISA+5}}{P_{SL}} = \frac{\rho_{SL,ISA+5}}{\rho_{SL}} \frac{T_{SL,ISA+5}}{T_{SL}}$$

or

$$\frac{\rho_{SL,ISA+5}}{\rho_{SL}} = \frac{P_{SL,ISA+5}}{P_{SL}} \frac{T_{SL}}{T_{SL,ISA+5}}$$

and since $P_{SL,ISA+5} = P_{SL}$

$$\frac{\rho_{SL,ISA+5}}{\rho_{SL}} = \frac{T_{SL}}{T_{SL,ISA+5}} = \frac{288.15}{293.15} = 0.98294$$

Thus, substituting into equation (C12),

$$\sigma_\rho = 0.98294(\sigma_\rho)_{ISA+5} \tag{C13}$$

From equation (C11), density altitude may be determined from

$$h_d = 1.4544 \times 10^5 \left[1 - \left(0.98294(\sigma_\rho)_{ISA+5}\right)^{0.235}\right] \tag{C14}$$

APPENDIX D - INPUTS REQUIRED BY GENHEL

This appendix outlines the steps required to calculate some of the inputs required to run *GenHel* for the results given in Section 4.

D1. EFFECT OF ATMOSPHERIC CONDITIONS

D1.1 Effect of Density and Temperature

Equation C3 gives

$$\sigma_\rho = \frac{\delta}{\theta}$$

Thus

$$(\sigma_\rho)_{max} = \frac{\delta_{max}}{\theta_{min}} \text{ and } (\sigma_\rho)_{min} = \frac{\delta_{min}}{\theta_{max}}$$

Therefore the maximum range in density would be obtained by combining the maximum pressure with the minimum temperature, and the minimum pressure with the maximum temperature.

To illustrate the variation of critical parameters due to atmospheric conditions, the maximum range in OAT and pressure was obtained from Ref. 1, i.e. OAT from 0°C to 50°C, ambient pressure from 28 inHg to 31.5 inHg.

Taking the maximum pressure and minimum temperature as an example, the pressure and density altitudes were determined for input to *GenHel* as follows:

For $P_a = 31.5$ inHg,

$$\delta = \frac{31.5}{29.92} = 1.0528$$

From equation C8, pressure altitude is given by

$$h_p = 1.4544 \times 10^5 \left(1 - 1.0528^{0.19026}\right) = -1431 \text{ ft}$$

Now, for OAT = 0°C,

$$\theta_{ISA+5} = \frac{273.15}{293.15} = 0.931776$$

Therefore,

$$(\sigma_\rho)_{ISA+5} = \frac{\delta_{ISA+5}}{\theta_{ISA+5}} = \frac{1.0528}{0.9318} = 1.1299$$

From equation C14, density altitude is given by

$$h_d = 1.4544 \times 10^5 \left[1 - (0.98294 \times 1.1299)^{0.235}\right] = -3631 \text{ ft}$$

D1.2 Effect of Ambient Temperature

The effects of OAT were illustrated by maintaining a constant density and varying the temperature. The sea-level ISA+5 density was chosen so that the temperature range (0°C to 50°C) would not result in a totally unrealistic range in pressure.

For $\rho = 0.002336$ slug/ft^3, $(\sigma_\rho)_{ISA+5} = 1$.

Now, for OAT = 0°C,

$$\theta_{ISA+5} = \frac{273.15}{293.15} = 0.931776$$

From equation C3,

$$\delta_{ISA+5} = (\sigma_\rho)_{ISA+5}\theta_{ISA+5} = 1 \times 0.931776 = 0.931776$$

Thus,

$$P_a = 0.931776 \times P_{SL,ISA+5} = 0.931776 \times 29.92 = 27.9 \text{ inHg}$$

The pressure altitude is given by equation C8,

$$h_p = 1.4544 \times 10^5 \left(1 - 0.931776^{0.19026}\right) = 1942 \text{ ft}$$

D2. EFFECT OF WEIGHT

Higher weights would be expected to have higher blade angles of attack, and thus increase the effects of compressibility, non-uniform inflow, and reverse flow. Two values of $W/(\sigma_\rho)_{ISA+5}$ were chosen to illustrate any variation of critical parameters due to different weights, namely 15000 lbf and 20000 lbf, e.g. for $W/(\sigma_\rho)_{ISA+5}$ = 20000 lbf, and maximum density, i.e. $(\sigma_\rho)_{ISA+5}$ = 1.1299, the actual weight input to *GenHel*, is W = 1.1299 x 20000 = 22598 lbf.

D3. EFFECT OF AMBIENT WIND

The effect of ambient wind was illustrated using four cases, namely hover, a forward true airspeed of 35 kn, ambient wind of 35 kn from port (`GAMHIC` = 270°), and ambient wind of 35 kn from starboard (`GAMHIC` = 90°).

The desired V of 35 kn was obtained by inputting V_{eq} calculated from

$$V_{eq} = V\sqrt{\sigma_\rho}$$

Note that the standard atmospheric density ratio is used because equivalent airspeed is given by an airspeed indicator calibrated for an ISA atmosphere. The standard atmospheric density ratio was determined from equation C13, i.e.

$$\sigma_\rho = 0.98294(\sigma_\rho)_{ISA+5}$$

Thus, for the maximum density conditions, i.e. $(\sigma_\rho)_{ISA+5}$ = 1.1299,

$$V_{eq} = 35\sqrt{0.98294 \times 1.1299} = 36.9 \text{ kn}$$

APPENDIX E - SURVEY OF AMBIENT SEA-LEVEL CONDITIONS

An initial survey was conducted of the ambient sea-level conditions likely to be encountered in the areas close to Australia, i.e. the Indian and South Pacific Oceans. The aim was to verify the suitability of the range of conditions that AMAFTU used when reporting FOCFT results (Refs 1 and 2). The range of conditions determined in this survey was applied to the *GenHel* predictions given in this report (Section 4).

Although it may reasonably be expected that FOCFTs would be conducted in oceans close to Australia, weight correction charts determined by AMAFTU must be applicable to all areas where the RAN may operate. A second survey was conducted of the ambient sea-level conditions likely to be encountered throughout the oceans of the world with the aim of determining the nominal maximum and minimum sea-level temperatures and pressures.

E1. Indian and South Pacific Oceans

Refs 15 and 16 show maps of the Indian and South Pacific Oceans, each containing about 40 small zones. Data recordings of monthly ambient conditions, including sea-level air temperature and pressure, were reported by ships of opportunity traversing these zones from 1850 through to 1970. The statistical data for each of the quantities recorded are given for each month and zone in the form shown in Fig. E1. These data were used to generate isotherms showing the mean ambient temperature and isobars showing the mean ambient pressure for each month, which have been overlayed on maps of the two oceans.

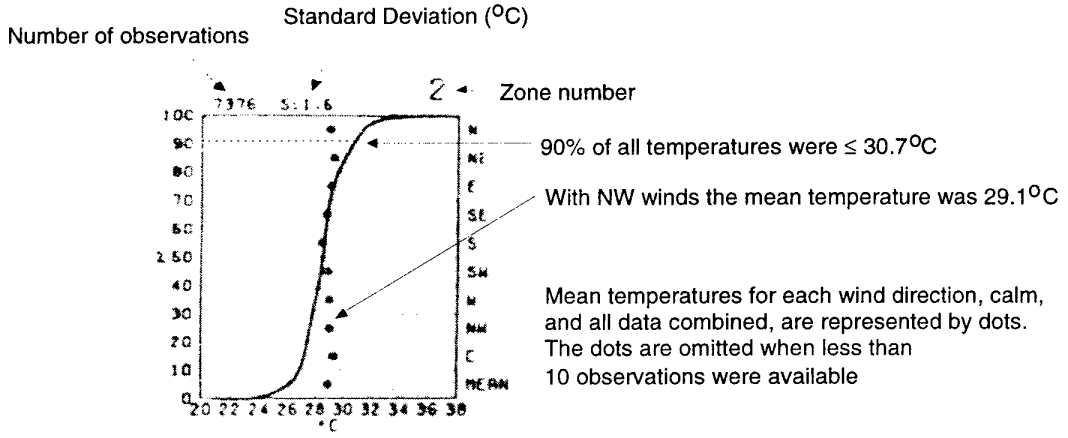

Figure E1. Typical Statistical Data for Sea-Level Ambient Air Temperature

The following procedure was undertaken to determine the minimum and maximum values of the ambient sea-level air temperature and pressure. Rather than examine each of the statistical data figures for all zones and each month (about 40 zones x 12 months x 2 quantities = 960 figures per ocean), the isotherms and isobars were first examined to determine the months which had the minimum and maximum mean values for these quantities. The detailed statistical figures were then examined for these months to determine the nominal minima and maxima.

Note that the nominal minima and maxima are based on the mean data together with variations about the mean determined by the standard deviation. Ref. 17 shows that for data having a normal distribution, about 99.7% of the data will lie in the range $\bar{x} \pm 3s$, where $\bar{x}$ is the mean value, and s is the standard deviation, i.e. the nominal minimum value of a given quantity will be $\bar{x} - 3s$ and the nominal maximum $\bar{x} + 3s$, although it is possible that minimum and maximum values outside of these ranges could occur.

The minimum and maximum mean values determined from the isotherms and isobars for both the Indian and South Pacific Ocean maps are summarised in Table E1. Since the minimum and maximum mean temperatures and pressures were found to occur from July to September, these months were chosen for detailed examination.

Table E1. Mean Ambient Sea-Level Temperatures and Pressures

Month	$(\overline{T}_a)_{min}$ (°C)	$(\overline{T}_a)_{max}$ (°C)	$(\overline{P}_a)_{min}$ (mb)	$(\overline{P}_a)_{max}$ (mb)
January	2	28	987.5	1025
February	4	28	990	1022.5
March	2	28	992.5	1022.5
April	2	28	987.5	1020
May	0	30	990	1020
June	0	30	987.5	1020
July	0	30	990	1027.5
August	0	30	987.5	1027.5
September	0	32	990	1025
October	0	30	990	1025
November	0	28	987.5	1025
December	2	28	987.5	1025

The zones through which the minimum and maximum isotherms and isobars passed were examined for July to September to determine the nominal maxima and minima. Results are summarised in Table E2 with the corresponding zone number shown in parenthesis where I indicates Indian Ocean and S indicates South Pacific Ocean. The approximate locations of the zones are given in Table E3.

Table E2. Maximum and Minimum Conditions

Month	$(T_a)_{min}$ (°C)	$(T_a)_{max}$ (°C)	$(P_a)_{min}$ (mb)	$(P_a)_{max}$ (mb)
July	-3 (S35)	36 (I1)	970 (S35)	1037 (I28)
August	-5 (S35)	35 (I1)	970 (S35)	1040 (S27)
September	-3 (S35)	35 (I1)	970 (S35)	1037 (I30)

Table E3. Approximate Location of Zones

Zone	Longitude, Latitude (deg)
I1	38E, 22N
I28	35E, 30S
I30	78E, 32S
S27	90W, 35S
S35	150W, 55S

The range of pressure indicated in Table E2 [970 mb (28.6 inHg) to 1040 mb (30.7 inHg)] is reasonably close to that given by Refs 1 and 2 [948 mb (28.0 inHg) to 1067 mb (31.5 inHg)], although the temperature range is significantly different. The maximum temperature of Refs 1 and 2 (50°C) is significantly higher than the nominal maximum of 36 °C given in Table E2 and the minimum temperature (0 °C) is not as low as the nominal minimum (-5 °C). Note

that, as indicated above, there is a low probability that the range of conditions defined by the nominal maxima and minima will be exceeded.

E2. Oceans of the World

Ref. 18 is a CDROM that includes a DOS program which reads a meteorological database to provide mean and standard deviation information on sea-level ambient temperature, sea-level atmospheric pressure, and various other quantities throughout the oceans of the world based on the data published in Refs 15, 16, and 19 to 25. As for Refs 15 and 16, the data originated from recordings reported by ships of opportunity traversing the global oceans from 1850 through to 1970.

The CDROM was used to obtain mean temperature or pressure information for a given month in terms of isotherms or isobars, then more detailed information was obtained for a selected geographical area in a 1° latitude by 1° longitude box. Fig. E2 shows a world map with isotherms labelled in °C for the month of January, and Fig. E3 shows similar information for the selected region 51N to 61N latitude and 136E to 158E longitude. A specific boxed area can be seen on Fig. E3, bounding 55N to 56N latitude and 136E to 137E longitude, with $\bar{x}$ and s data for various quantities in this area shown on the right. The values of $\bar{x}$, $\bar{x} \pm s$, $\bar{x} \pm 2s$, and $\bar{x} \pm 3s$ for the ambient air temperature in this specific area can be seen at the bottom of the figure. A similar procedure may be performed for sea-level pressure data.

In this way, statistical information was gathered for the ambient sea-level temperature and pressure, and the nominal minima and maxima conditions were determined, as shown in Table E4. Note that the pressure range (942.5 to 1057.6 mb) is closer to the range used in Refs 1 and 2 (948 to 1067 mb) than that found in Section E1 (970 to 1040 mb), but the lower end of the temperature range in particular (-50°C) is considerably different than Refs 1 and 2 (0°C) and Section E1 (-5°C). As previously discussed, there is a low probability that the range of conditions defined by the nominal minima and maxima will be exceeded.

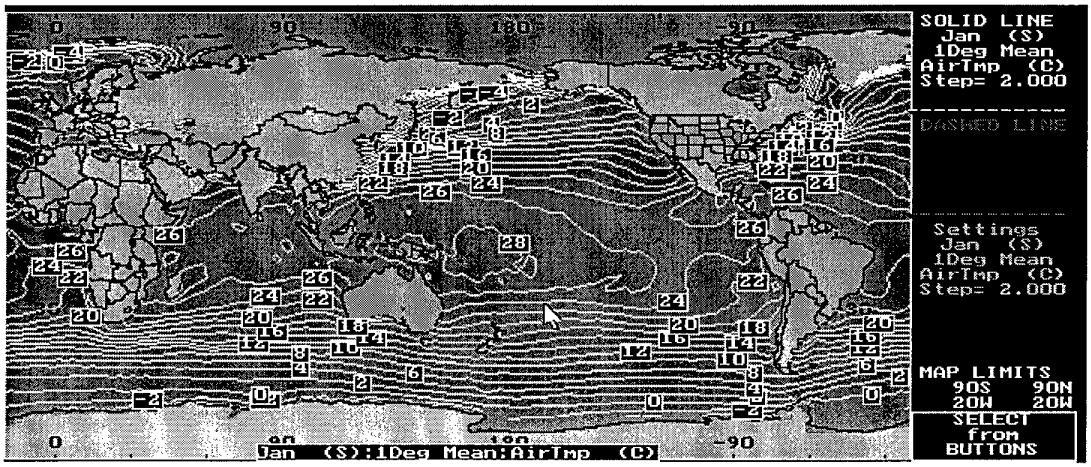

Figure E2. Mean Sea-Level Ambient Air Temperature for January

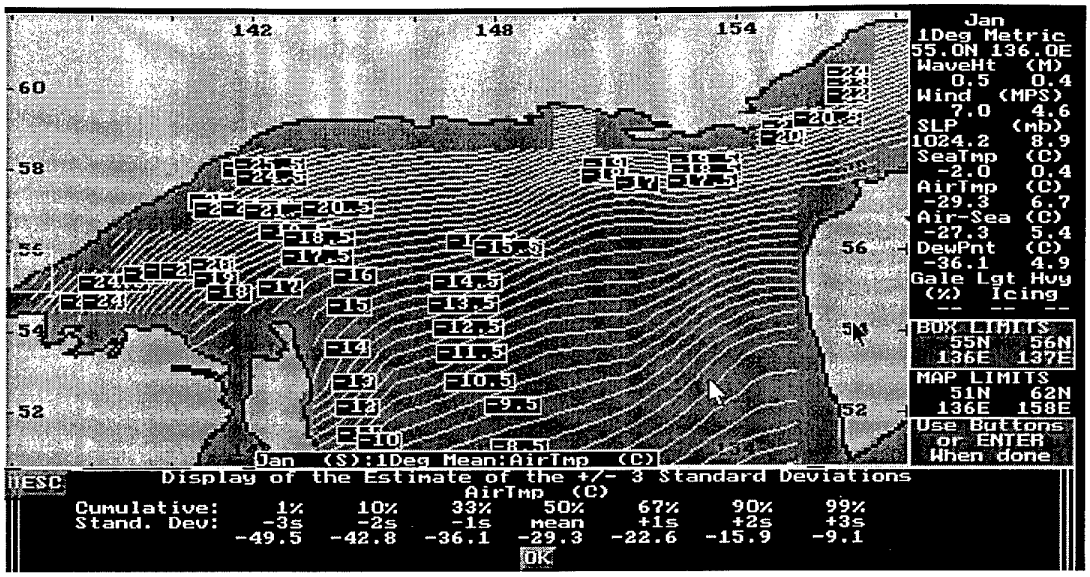

Figure E3. Sea-Level Ambient Temperature Statistics for a Specific Region

Table E4. Nominal Maxima and Minima Sea-Level Conditions

Longitude	Latitude	Month	Minimum	Mean	Maximum
				T_a (°C)	
55N-56N	136E-137E	Jan	-49.5	-29.3	-9.1
28N-29N	48E-49E	Jul	25.5	33.4	41.4
				P_a - mb (inHg)	
65S-66S	116E-117E	Sep	942.5 (27.83)	979.8 (28.93)	1017.0 (30.03)
63N-64N	171W-172W	Jan	977.1 (28.85)	1017.4 (30.04)	1057.6 (31.23)

DISTRIBUTION LIST

The Referred Weight Flight Test Technique Applied to First of Class Flight Trials

A.M. Arney

AUSTRALIA

DEFENCE ORGANISATION

Task Sponsor Director of Aviation Engineering - Navy

S&T Program

Chief Defence Scientist
FAS Science Policy } shared copy
AS Science Corporate Management
Director General Science Policy Development
Counsellor Defence Science, London (Doc Data Sheet)
Counsellor Defence Science, Washington (Doc Data Sheet)
Scientific Adviser to MRDC Thailand (Doc Data Sheet)
Director General Scientific Advisers and Trials/Scientific Adviser Policy and Command (shared copy)
Navy Scientific Adviser
Scientific Adviser - Army (Doc Data Sheet and distribution list only)
Air Force Scientific Adviser
Director Trials

Aeronautical and Maritime Research Laboratory
Director

Chief of Air Operations Division
Research Leader, Aircraft Performance
Research Leader, Flight Systems
Head Helicopter Operations (6 copies)
Head Operations and Performance Analysis
A.M. Arney (2 copies)

DSTO Library
Library Fishermens Bend
Library Maribyrnong
Library Salisbury (2 copies)
Australian Archives
Library, MOD, Pyrmont (Doc Data sheet only)

Forces Executive
Director General Force Development (Sea)
Director General Force Development (Land) (Doc Data Sheet)

Navy

SO (Science), Director of Naval Warfare, Maritime Headquarters Annex, Garden Island, NSW 2000 (Doc Data Sheet only)
Aircraft Maintenance and Flight Trials Unit
CO HMAS Albatross
Office of Naval Attache, Washington
RAN Tactical School, Library
Superintendant Naval Aircraft Logistics

Army

ABCA Office, G-1-34, Russell Offices, Canberra (4 copies)
CO 5 RGT, Townsville
School of Army Aviation, Oakey

Air Force

Aircraft Research and Development Unit
Scientific Flight Group
Library

S&I Program

Defence Intelligence Organisation
Library, Defence Signals Directorate (Doc Data Sheet only)

B&M Program (libraries)

OIC TRS, Defence Regional Library, Canberra
Officer in Charge, Document Exchange Centre (DEC), 1 copy
*US Defence Technical Information Centre, 2 copies
*UK Defence Research Information Center, 2 copies
*Canada Defence Scientific Information Service, 1 copy
*NZ Defence Information Centre, 1 copy
National Library of Australia, 1 copy

UNIVERSITIES AND COLLEGES

Australian Defence Force Academy
Library
Head of Aerospace and Mechanical Engineering
Deakin University, Serials Section (M list), Deakin University Library, Geelong, 3217
Senior Librarian, Hargrave Library, Monash University
Librarian, Flinders University

OTHER ORGANISATIONS

NASA (Canberra)
AGPS

OUTSIDE AUSTRALIA

ABSTRACTING AND INFORMATION ORGANISATIONS

INSPEC: Acquisitions Section Institution of Electrical Engineers
Library, Chemical Abstracts Reference Service
Engineering Societies Library, US
Materials Information, Cambridge Scientific Abstracts, US
Documents Librarian, The Center for Research Libraries, US

INFORMATION EXCHANGE AGREEMENT PARTNERS

Acquisitions Unit, Science Reference and Information Service, UK
Library - Exchange Desk, National Institute of Standards and Technology, US

TTCP COLLABORATIVE PARTNERS

Canada

National Research Council, Ottawa
R. Thompson (Canadian NL TTCP HTP-6)
S. Zan
University of Toronto
L.D. Reid

United Kingdom

Defence Research Agency, Bedford
G.D. Padfield
B. Lumsden
Defence Research Agency, Farnborough
A.F. Jones (UKNL TTCP HTP-6)
Rotary Wing Performance Section, DTEO Boscombe Down
R. Finch
MOD DGA, Aircraft Support Executive, London
P. Symonds

United States

US Army Aeroflightdynamics Directorate, Ames Research Center
W.G. Bousman (USNL TTCP HTP-6)
Naval Air Warfare Center, Aircraft Division, Patuxent River
J.W. Clark, Jr (TTCP HTP-6)
J. Funk
D. Carico
J. McCrillis
L. Trick
Naval Air Warfare Center, Aircraft Division, Lakehurst
H. Fluk

SPARES (10 copies)

Total number of copies: 88

DEFENCE SCIENCE AND TECHNOLOGY ORGANISATION
DOCUMENT CONTROL DATA

1. PRIVACY MARKING/CAVEAT (OF DOCUMENT)

2. TITLE

The Referred Weight Flight Test Technique Applied to First of Class Flight Trials

3. SECURITY CLASSIFICATION (FOR UNCLASSIFIED REPORTS THAT ARE LIMITED RELEASE USE (L) NEXT TO DOCUMENT CLASSIFICATION)

Document	(U)
Title	(U)
Abstract	(U)

4. AUTHOR(S)

A.M. Arney

5. CORPORATE AUTHOR

Aeronautical and Maritime Research Laboratory
PO Box 4331
Melbourne Vic 3001

6a. DSTO NUMBER	6b. AR NUMBER	6c. TYPE OF REPORT	7. DOCUMENT DATE
DSTO-TR-0509	AR-010-178	Technical Report	April 1997

8. FILE NUMBER	9. TASK NUMBER	10. TASK SPONSOR	11. NO. OF PAGES	12. NO. OF REFERENCES
M1/9/299	NAV 95/183	DAVENG-N	34	25

13. DOWNGRADING/DELIMITING INSTRUCTIONS

None

14. RELEASE AUTHORITY

Chief, Air Operations Division

15. SECONDARY RELEASE STATEMENT OF THIS DOCUMENT

Approved for public release

OVERSEAS ENQUIRIES OUTSIDE STATED LIMITATIONS SHOULD BE REFERRED THROUGH DOCUMENT EXCHANGE CENTRE, DIS NETWORK OFFICE, DEPT OF DEFENCE, CAMPBELL PARK OFFICES, CANBERRA ACT 2600

16. DELIBERATE ANNOUNCEMENT

No Limitations

17. CASUAL ANNOUNCEMENT Yes

18. DEFTEST DESCRIPTORS

Sikorsky helicopters, flight tests, flight trials, flight simulation, mathematical models, referred weight

19. ABSTRACT

The referred weight flight test technique has been used by the RAN to establish Ship Helicopter Operating Limits for a number of years. This technique involves keeping the referred weight, defined as aircraft weight divided by density ratio, constant for a given flight test. The validity of using this technique has been questioned within the RAN, specifically with respect to its relevance and application to power and flight control margins. This report illustrates the relationships between power requirements, flight control positions, and referred weight by first using simplified equations to derive the mathematical relationships. To verify these relationships, the simulation code *GenHel*, which allows for many of the complex factors ignored in deriving the simplified equations, has been applied over a wide range of conditions. Results suggest that the referred weight technique is valid for conditions typically encountered during First of Class Flight Trials.